Heterogeneous Approaches for Localization based on Received Signal Strength Indicator

Han Zhaoyang

A DISSERTATION

SUBMITTED IN FULFILLMENT OF THE REQUIREMENTS

FOR THE DEGREE OF DOCTOR OF PHILOSOPHY

IN COMPUTER SCIENCE AND ENGINEERING

Graduate Department of Computer and Information Systems

The University of Aizu

2022

The dissertation titled

Heterogeneous Approaches for Indoor Localization based on Received Signal Strength Indicator

by

Han Zhaoyang

is reviewed and approved by:

Main referee	
Senior Associate Professor	Aug 5, 2022
SU Chunhua	Su Chunhua (SU)
Senior Associate Professor	
NAKAMURA Akihito	(中村) Aug 16, 2022
Senior Associate Professor	
ZHU Xin	Zhu Xin (朱) Aug. 17, 2022
Associate Professor	
YEN Neil Yuwen	Neil Yen (嚴) Aug. 16. 2022

THE UNIVERSITY OF AIZU

September 2022

Contents

List of Figures

List of Tables

List of Abbreviations

GPS	Global Positioning System
RSS	Received Signal Strength
ToA	Time of Arrival
SISO	Single Input and Single Output
SNR	Signal-to-Noise-Ratio
MIMO	Multi Input and Multi Output
RTT	Round-Trip Time
TDOA	Time Difference of Arrival
CIR	Channel Impulse Response
CFR	Channel Frequency Response
IFT	Inverse Fourier Transform
CSI	Channel State Information
OFDM	Orthogonal Frequency Division Multiplexing
RFID	Radio Frequency Identification
DFL	Device-Free Localization
IoT	Internet-of-Things
AP	Anchor Points
DNN	Deep Neural Network
CNN	Convolutional Neural Network
SRC	Sparse-Representation-Classification

Abstract

Although Global Positioning System (GPS) technique has been widely used in the field of outdoor localization, GPS signals cannot be effectively transmitted in a complex indoor environment. Positioning and navigation cannot be performed in typical situations such as indoor emergency occurrence location determination, shopping mall guides, and intelligent service robot fixed-point services. To alleviate issues brought by the GPS position, related researchers utilized various signals (e.g., WiFi, ZigBee and RFID) to achieve more accurate indoor target positioning. However, most proposed indoor localization algorithms are complex and costly, and do not consider some specific circumstances where the attached device are unavailable. In this dissertation, to address the existing problems, we propose a series of indoor localization frameworks in terms of novel scene modeling and algorithm improvement.

This dissertation provides triple research focuses. Firstly, we propose a new algorithm to integrate indoor target positioning and communication based on the features of WiFi signal. Given in some scenarios, the target may not expect to be equipped with extra devices. Therefore, we formulate device-free localization issue as the classification problem and exploit a log regularizer in the objective function for classification. Finally, to increase the accuracy of device free localization, we utilize convolution neural networks (CNN) to handle the classification problem. The organization and contribution of this dissertation are summarized as follows.

Chapter 1 (Introduction) introduces the basic background of indoor and device free localization. Subsequently, the related techniques used to tackle the localization problem are presented briefly.

Chapter 2 (WiFi-based Indoor Positioning and Communication: Empirical Model and Theoretical) proposes a new algorithm to integrate indoor target positioning and communication based on WiFi signals. The RSS and CSI values of WiFi signal are used for target location and indoor wireless channel modeling, respectively. The experimental results show that the proposed positioning algorithm can achieve localization within the ideal accuracy range.

Chapter 3 (Device-Free Localization via Sparse Coding with Log-Regularizer)considers the device free scenario for indoor localization. Therefore,in this chapter, we ex-

ploit a new log regularizer in the sparse coding objective function for classification. With taking the distinctive ability of log-regularizer to measure sparsity, the proposed approach can achieve an accurate localization process with robust performance in the challenging environments. Even if the input data is severely polluted by noise with a level of SNR = -10 dB, our algorithm can still keep a high accuracy of 99.4%.

Chapter 4 (Image Processing-based indoor device-free localization) presents a machine learning-oriented device free localization method by using image processing method. We convert the received signal strength (RSS) signals into image pixels. The localization problem is then formulated as an image clarification problem. To well handle the variant RSS images, a deep convolutional neural network is then structured for classification. In particular, we simulated and expanded the amount of data for the scenarios where the sensors may be dropped or the data may be tampered by attackers, and trained the proposed CNN model from scratch with these data in advance. The experimental results show that our system still works properly and has high localization accuracy in case of the above scenarios.

Chapter 5 concludes the major contributions of this research and illustrates some potential directions for future work.

概要

全地球測位システム（GPS）技術は、屋外の位置測定の分野で広く利用されているが、複雑な屋内環境では GPS 信号を効果的に伝達することができない。屋内の緊急発生位置の決定、ショッピングモールのガイド、インテリジェントサービスロボットの特定サービスなどの典型的な応用では、位置測定とナビゲーションが行えなくなる。これらの問題を解決するために、多くの研究者はより正確な屋内ターゲットの位置測位を達成するために、様々な信号（例えば、WiFi、ZigBee、RFID）を利用した。しかし、提案されている屋内測位アルゴリズムのほとんどは、構成が複雑で実装コストが高く、接続されたデバイスが利用できないなどの特定状況を考慮していない。本論文では、既存の未解決問題を対処するため、新規なシーンモデリングを提案し、位置決定アルゴリズム改良し、一連の屋内測位フレームワークを提案する。

本論文では、我々は以下の 3 つの研究課題を着目する。１つ目は WiFi 電波の特徴に基づき、屋内ターゲットの測位と通信を統合する新しいアルゴリズムを提案する。２つ目研究課題は WiFi を搭載していないシナリオを想定して追加対策を提案する。そこで、デバイスフリー定位問題を分類問題として定式化し、分類のための目的関数に対数正則化器を用いることで、デバイスフリー定位を実現する。最後に、3 つ目の研究課題はデバイスフリー局在化の精度を向上させるために、畳み込みニューラルネットワーク（CNN）を分類問題の処理に利用した手法を提案する。本論文の構成と貢献は以下のようにまとめられる。

第 1 章の「はじめに」では、屋内およびデバイスフリー定位に関する基本的な背景を紹介する。続いて位置測位問題に取り組むために使用される関連技術などの背景知識を紹介する。

第 2 章「WiFi を利用した屋内測位・通信。実証モデルと理論」では、WiFi 電波に基づく屋内目標位置と通信を統合するための新しいアルゴリズムを提案する。WiFi 電波の RSS と CSI 値は、それぞれターゲットの位置と屋内無線チャネルのモデリングに使用される。実験結果から、提案する測位アルゴリズムは理想的な精度範囲での測位を実現できることを示す。

第 3 章「対数正則化器を用いたスパース符号化によるデバイスフリーな位置特定」では、屋内位置測位についてデバイスフリーのシナリオを考える。そこで、本章では、分類のためのスパースコーディング目的関数において、新し

い対数正則化器を導入して利用する。我々の提案手法は、対数正則化器の特徴であるスパース性を利用することで、厳しい環境下でもロバストな性能で正確な定位処理を実現する。また、入力データが SNR=-10dB のノイズに汚染されても、99.4% という高い精度を維持することが可能にする。

第 4 章「画像処理に基づくデバイスレス屋内測位」では、画像処理手法を用いた機械学習指向のデバイスフリー位置測位手法を紹介する。受信信号強度（RSS）を画像ピクセルに変換する。そして、局在問題は画像分類問題として定式化を行う。この問題に対して、深層畳み込みニューラルネットワークを構築して分類を行う。特に、センサーが落下したり、攻撃者によってデータが改ざんされたりするシナリオを想定してシミュレーションを行い、データ量を拡張し、これらのデータを用いて提案する CNN モデルを事前に一から学習させました。実験の結果、上記のようなシナリオの場合でも、本システムは正常に動作し、高い位置特定精度を有することが確認されました。

第 5 章では、本研究の主な成果を結論付け、今後の研究の方向性を示す。

Acknowledgment

Many people have given me kind and careful help. I want to thank these people from the bottom of my heart.

First, I would like to thank my supervisor, Professor Chunhua Su, who is very knowledgeable and sincere. He always gave me the wisest advice when I was most confused. Professor Su is kind and always easy to get along with. In addition to studying and researching, Mr. Su would also take us to Japan to experience exotic places and cultures.

Secondly, I would like to thank the other defending professors here: Prof. Nakamura Akihito, Prof. Zhu Xin, and Prof. Yen Neil Yuwen. Mr. Nakamura always had a kind face, and besides academic guidance, Mr. Nakamura also gave me some kind and detailed advice about other aspects of my thesis. Prof. Zhu is a kind teacher who always found problems in my thesis and defense process and gave reasonable suggestions. Professor Neil is a dynamic and energetic teacher who always inspires and motivates me. Thank you to all of the above teachers. Thank you for all the help I received from my teachers.

I would also like to thank my lab members, including those who have graduated from the lab. They have made my research path less lonely. They always help and support me sincerely behind my back. They have always helped me with academics and life. I miss the time with you guys. I am lucky to have met you all, making my study more hopeful and my life in a foreign country more smiling. Thank you all.

Finally, I would like to give my highest respect and love to my family members. Thank you for your silent dedication to me. Thank you for your most selfless love for me. I love you all forever.

Publications

This thesis is based on the following published papers during my Ph.D. study at the University of Aizu:

1. **Z Han,** Z Wang, H Huang, L Zhao, C Su (2022). WiFi-Based Indoor Positioning and Communication: Empirical Model and Theoretical Analysis. Wireless Communications and Mobile Computing. DOI:10.1155/2022/2364803.

2. **Z Han,** L Lin, Z Wang, Z Lian, C Qiu, H Huang, L Zhao, C Su (2022). CNN-Based Attack Defense for Device-Free Localization. Mobile Information Systems. DOI:10.1155/2022/2323293

3. **Z Han,** C Su, S Ding, H Huang, L Zhao (2019). Device-free localization via sparse coding with log-regularizer. 2019 IEEE 10th international conference on awareness science and technology (iCAST). DOI:10.1109/ICAwST.2019.8923592.

Chapter 1

Introduction

1.1 Wireless localization

In recent years, with the rapid development of a new generation of mobile communication technology, mobile network technology has gradually improved and matured. At the same time, the demand for location services continues to increase. Currently, many technologies can meet indoor positioning requirements, and their implementation's complexity and cost vary. Under the premise of ensuring a certain accuracy, whether the wireless network can make full use of the wireless network and at the same time give full play to the communication capability is a question worthy of consideration and research.

At this stage, outdoor positioning technology has developed very maturely and is basically complete. With its good performance, Global Positioning System (GPS) technology has been accepted and widely used. However, because GPS positioning technology mainly relies on signals propagating in the air, the complex environment indoors hinders the signal's propagation in the air, thus limiting the applicability of GPS indoors. In order to meet the huge demand of indoor positioning technology, many researchers have used wireless communication technologies such as ultrasonic[1], infrared[2], sensor, RFID, WiFi, UWB, Bluetooth, etc. to achieve the goal of indoor positioning. The characteristics of low cost and widely using make WiFi a more promising indoor positioning technology.

1.2 Indoor localization

The typical indoor localization techniques can be categorized into ultrasonic, infrared, sensor, RFID, WiFi, UWB and Bluetooth. The ultrasonic positioning is simple and the measurement results have high accuracy. However, the experiment results are easy to be affected by NLOS, the hardware requirements are high and the cost is high. The infrared positioning does not spread during transmission. Moreover, NLOS affects the positioning result, and the transmission distance is limited. Although the system structure and measurement principle of RFID positioning are simple, its accuracy is directly proportional to system complexity. UWB positioning consumes low power and provides strong anti-interference, and low system complexity. However, the requirement of strict clock synchronization at the sender and receiver, and the hardware cost is high. WiFi positioning

only requires simple equipment, low cost and low implementation difficulty, but experiment performance owns low accuracy and lacks of effective use of signals.

Furthremore, based on the RSS value of the WiFi signal, the related indoor positioning technology development has achieved the following achievements. Huang et al. [2] first analyzed the sources of positioning errors of moving objects based on RSS algorithm, and based on this, proposed a weighted filtering algorithm based on motion speed and Kalman filtering. The new fusion algorithm is better than traditional Kalman filtering algorithms [3]. The error is small, but there are still problems of low positioning accuracy and low reliability; Ma et al. [4] put forward the two-phase positioning idea of online and offline on the traditional fingerprint positioning algorithm. The experimental results show that the weighted fusion of the two positioning results is more accurate than the WKNN and joint probability algorithm, but the cost of this algorithm in actual application is greater and it is more difficult to implement; Wang et al. [5] proposed an improved algorithm based on RSS fingerprint library in view of the limitations of traditional WKNN algorithm. Although the improved algorithm improves the positioning accuracy to some extent, there are still problems that the RSS fingerprint database is difficult to set up and the filtering is more complicated; Deng et al. [6] proposed an improved fusion algorithm based on Kalman filtering. Although the positioning accuracy of the algorithm is higher than that of the WiFi-based positioning algorithm alone, there are still deficiencies such as insufficient applicability. Hsieh et al. [7] put forward the idea of using deep learning to solve the RSS and CSI values based on WiFi signals. Although the algorithm has improved accuracy compared to traditional positioning algorithms, the complexity of the algorithm is too high and the implementation is difficult. In order to solve the problem of inaccurate RSS data source, Yu et al. [8] proposed an effective algorithm for extracting RSS information. Experimental results show that the positioning accuracy of the algorithm can reach 1.5m, but there are still some shortcomings such as large workload and low accuracy. Lembo [9] analyzed the RSS signal measurement at the physical structure level, and finally combined the neural network algorithm to improve the positioning accuracy. However, this method also has the disadvantages of a single mode and insufficient flexibility. Guo et al. [10] proposed a RTT-RSS ranging algorithm based on WiFi signals in the scenario where a smartphone is used indoors. The experimental results of the algorithm show that the accuracy of the algorithm can reach 1.435m. However, the algorithm is still insufficient in scene applicability and complexity of implementation. Shu et al. [11] proposed a prediction algorithm based on indoor WiFi data's queuing time. The experimental results show that the wheel model proposed by the author is basically consistent with the theoretical analysis. It has strong applicability, but it has the disadvantage of low accuracy. Yang et al. [12] proposed a high-resolution TOA estimation algorithm and a new AOA estimation algorithm with the help of the new algorithm. Although the experimental results are improved compared with the traditional algorithms, they have the disadvantage of requiring high experimental conditions. In terms of communication function which based on the value of CSI, the wireless channel system transmission function is analyzed by modeling the indoor wireless channel to complete the communication function. After analyzing the classical wireless channel modeling method, Michelson et al. [13] put forward the idea of wireless channel modeling based on a variety of factors based on the needs of actual life.

The idea is a good balance between theory and practice's relationship; Kumar et al. [14] proposed a wireless channel model in the indoor single-transmit and single-receive scenario. The test results show that although the model can play an important role in broadband mobile communications, it also has the disadvantages of poor applicability and inflexibility; Xu et al. [15] modeled the wireless channel under the conditions of multiple transmissions and multiple receptions. Although the model can reflect the state of the wireless channel to a certain extent, there are still the disadvantages that the model is not accurate enough; Kalachikov et al. [16] theoretically used a matrix analysis method to analyze the model of the wireless channel in the MIMO scene. The results show that the model designed by the author is more in line with the characteristics of actual measured values than the traditional model. The disadvantage is that the system complexity is too high. , The amount of calculation is too large, it is more difficult to implement; Stridh [17] modeled the MIMO channel at 5.8GHz. The experimental results show that the model established by the author basically conforms to the objective law. The disadvantage is that the model is not applicable and the complexity is high. Liu et al. [18] modeled the wireless channel from the perspective of a Markov chain. The experimental results show that although the model can meet the experimental requirements under certain conditions, it also has the problem of insufficient accuracy.

1.3 Device free localization

Device free localization does not require the target to carry any mobile devices, sensors, tags or other electronic equipment and is relatively easy and inexpensive to implement. Due to these advantages, the use of portable device targeting can be used in border security, disaster relief, entry check side and smart home. In disaster rescue, the sensor nodes are quickly deployed in the disaster area, and the specific location of the trapped person is quickly located through the portable device targeting technology, which greatly reduces the time spent on search and rescue, and improves the search and rescue efficiency of the search and rescue personnel, ultimately allowing the trapped person to get out of the danger area in time and reducing casualties. For example, in the event of a fire in a building, the use of a wireless sensor network, either pre-deployed or temporarily deployed around the building, can help searchers to quickly identify the location of trapped persons in a building full of smoke and flames, thus enabling them to be rescued more quickly. Another application of portable device targeting technology is border security. For example, a portion of low-power sensor nodes are deployed in advance in a long border area, and when a stowaway enters the detection area, the sensor nodes are triggered to upload detection data, and the coordinates of the stowaway can be accurately located by means of the device free targeting technology, so that the stowaway can be monitored and apprehended in time.

Chapter 2

WiFi-based Indoor Positioning and Communication: Empirical Model and Theoretical Analysis

2.1 Introduction

2.1.1 Background

With the rapid development of the wireless communication, mobile internet technology has been steadily matured and gradually completed in recent years. Since positioning service is able to provide more accurate time information and space information, improve user experience, ensure the property safety of people in all walks of life, and promote the development of the information society, it can be regarded as one of the most successful applications of the mobile internet technology, which has been paid more and more attention.

On the one hand, outdoor positioning technology has made great progress, where Global Positioning System (GPS) technology has been widely used due to its performance of low latency, ideal accuracy and high resolution. However, since GPS positioning technology severely relies on signals propagating in the air, the complex environment indoors hinders the signal's propagation, GPS's applicability is severely limited in the indoors environment. On the other hand, as for the indoor positioning aspect, there are many types of technologies to realize the indoor positioning, such as ultrasonic [19], infrared [20], sensor [21], RFID [22], WiFi [23], UWB [23], Bluetooth [24], etc., whose comparison of advantages and limitation are presented in Table I.

Note that despite different positioning method is with different complexity and cost of implementation, low cost and widely use characteristics make WiFi-based approach a more promising indoor positioning technology. Furthermore, though most algorithms and technologies can achieve the goal of indoor positioning, how to maximize the indoor wireless signal's utilization, e.g., joint positioning and communication with indoor wireless signal, while keeping certain positioning accuracy has not been fully considered and investigated.

Table 2.1: Comparison of different positioning technology.

Name	Advantages	Limitations
Ultrasonic positioning	The equipment is simple, and the measurement results have high accuracy.	Affected by NLOS, the hardware requirements are high, and the cost is high.
Infrared positioning	Does not spread during transmission.	Affected by NLOS, the transmission distance is limited.
RFID positioning	The system structure and measurement principle are simple.	Accuracy is directly proportional to system complexity.
UWB positioning	Low power consumption, strong anti-interference, and low system complexity.	Requires strict clock synchronization at the sender and receiver, and the hardware cost is high.
WiFi positioning	Simple equipment, low cost, and common implementation difficulty	Low accuracy and lack of effective use of signals

2.1.2 Related works

As one indispensable metric of the WiFi signal, Received Signal Strength (RSS) could reflect the geometry distribution of the transmitted signal, where the larger RSS value is, the closer the target is to the transmitter. Based on such theory, the WiFi-based indoor positioning approach is put forward, which relates the target's position with the RSS value by establishing the WiFi-based signal fingerprinting databased. At this time, the position of the target can be estimated by comparing the current RSS value with the established fingerprinting. Up to now, lots of efforts have been made on the RSS-based WiFi indoor positioning technology, for example, Huang et al. [2] analyzed the reasons for moving objects' positioning errors in the RSS-based positioning approach, where a motion speed and Kalman filtering-based weighted filtering algorithm is proposed. The new fusion algorithm performs better than traditional Kalman filtering algorithms, whose positioning error can be greatly reduced [3]. Ma et al. [4] put forward the online and offline positioning method based on the traditional fingerprint positioning algorithm, whose experimental results show that the weighted fusion of the two positioning results can be more accurate than the WKNN and joint probability algorithm. Given the limitations of the traditional WKNN algorithm, Wang et al. [5] proposed an improved algorithm based on the RSS fingerprint database, where the positioning accuracy can be enhanced by the proposed algorithm to some extent. In [6], Deng et al. proposed an improved fusion algorithm based on Kalman filtering, and the positioning accuracy of the proposed algorithm is higher than that of the WiFi-based positioning algorithm. In [7], Hsieh et al. used the deep learning method to derive the RSS and CSI values of WiFi signals, by which the positioning accuracy can be enhanced compared to the traditional positioning algorithms. Yu et al. [8] solved the problem of inaccurate RSS data sources, where a practical algorithm for extracting RSS information is proposed. Besides, experimental results show that the positioning accuracy of the algorithm can reach 1.5m. Lembo et al. [9] gave the detailed analysis on the RSS measurement at the physical structure level and combined the neural network algorithm to improve positioning accuracy, which is proved to meet the needs of ideal positioning errors compared with the typical

baselines. In the scenario where a smartphone is used indoors, Guo et al. put up an RTT-RSS-based ranking algorithm with WiFi signals, and the experiment results show that the algorithm's accuracy can reach 1.435m. Shu et al. [11] proposed a prediction algorithm based on indoor WiFi data's queuing time, whose experimental results show that the proposed wheel model is consistent with the theoretical analysis and has strong applicability. Yang et al. [23] proposed a high-resolution Time of Arrival (ToA) estimation algorithm, and compared with the traditional algorithms, the experimental results of the positioning performance are improved.

In terms of communication function of the WiFi signal, it can be realized based on the CIS information. Specifically, with the help of CIS value, after modeling the indoor wireless channel, the transmission function of the wireless communication system can be derived to complete the communication function. So far, many researchers have devoted themselves to the CSI-based communication realization, for example, in [13], after analyzing the classical wireless channel modeling method, Michelson et al. put forward the multiple factors-based wireless channel modeling algorithm due to the needs in real life. And the experiment results show that the proposal can trade off theory and practice of communication function well. Kumar et al. [14] proposed a wireless channel model in the indoor Single Input and Single Output (SISO) scenario, where the experiments results show that the proposed model can play an essential role in broadband mobile communications. Xu et al. [15] modeled the wireless channel under the conditions of multiple transmissions and multiple receptions, and experiments proves that the model can reflect the state of the wireless channel to a certain extent. Kalachikov et al. [16] used a matrix analysis method to analyze the wireless channel model in the Multi Input and Multi Output (MIMO) scene in theory. The results show that the designed model is more in line with the characteristics of actual measured values than the traditional model. Stridh et al. [17] modeled the MIMO channel at 5.8GHz, where the experimental results show that the established model is feasible. Liu et al. [18] gave the model of the wireless channel from the perspective of a Markov chain, and the experimental results show that although the model can meet the practical requirements under various parameter settings.

In summary, despite RSS-based approaches can realize the indoor positioning with WiFi signal, the tradeoff between high positioning accuracy, smaller positioning error, and less implement cost is difficult to achieve. Moreover, the wireless channel function can be estimated with the CSI information, but the proposed model has not been comprehensively analyzed and proofed in theory. Therefore, form the viewpoints of numerical results and theorical analysis, the joint indoor positioning and communication based on RSS and CSI of WiFi signal has not been taken into consideration, which would be the work of this paper.

2.1.3 Motivation and contribution

Based on the above analysis, to address the tricky problem, where the complexity and implementation cost, and indoor wireless signal's utilization are paid little attention by the state-of-art efforts on indoor positioning, this paper aims at proposing one WiFi-based indoor positioning and communication scheme, where RSS information is used to achieve the positioning goal, and communication func-

tion is realized with the help of CSI information. In summary, the main contribution of this paper can be summarized as the following threefold:

1) To achieve the indoor positioning goal with WiFi technology, the RSS information is utilized, where an empirical model is established to replace the traditional fingerprinting database with the curve fitting approach.

2) To realize the WiFi-based indoor communication target, we establish the wireless channel modeling under the SISO and OFDM-based MIMO scenarios respectively, where the proposal is proved to be feasible given the environment noise existence.

3) To evaluate the feasibility and performance of the proposal, numerical experiments are conducted, and the results have shown that when compared with other benchmarks, the proposed method can achieve smaller positioning error with less implement cost.

2.1.4 Outline of the paper

The rest of this paper is organized as follows. In the Section II, the typical indoor positioning technologies are introduced from three aspects, i.e., ToA-based positioning, TDoA-based positioning, and CSI-based positioning. Section III establishes the system model and formulates the problem, where RSS-based positioning model and Kalman filtering model are detailed. Section IV gives the empirical model-based indoor positioning scheme with WiFi, where the collection and process steps of RSS data are presented. In section V, the theoretical analysis for WiFi-based indoor communication is given, where the derivations of wireless channels are detailed from SISO, and OFDM-based MIMO scenarios respectively. The numerical experiments are conducted in Section VI, where indoor positioning performance is evaluated with numerical results, and indoor communication function is verified in theory. Finally, a brief conclusion is given to summarize the whole paper in Section VII.

2.2 Typical indoor positioning technology

2.2.1 ToA-based indoor positioning

The Round-Trip Time (RTT) refers to the time between the transmitter and the receiver. With the help pf RTT, the distance between the transmitter and the receiver can be obtained by multiplying half of RTT and the signal propagation speed. Fig. 2.1. shows the principle of Time of Arrival (ToA)-based positioning. As shown in Fig. 2.1., MP indicates the object's position to be determined, AP_1, AP_2, and AP_3 indicate three access points respectively. According to the measured RTT value, the values of d_1, d_2, and d_3 can be calculated. Denote the positioning information of AP_1, AP_2, AP_3, and MP as $AP_1(x_1, y_1), AP_2(x_2, y_2), AP_3(x_3, y_3), MP(x, y)$ respectively. Hence, the position of MP can be solved by combining the following equation:

$$\begin{aligned}(x-x_1)^2+(y-y_1)^2&=d_1^2\\(x-x_2)^2+(y-y_2)^2&=d_2^2\\(x-x_3)^2+(y-y_3)^2&=d_3^2\end{aligned} \tag{2.1}$$

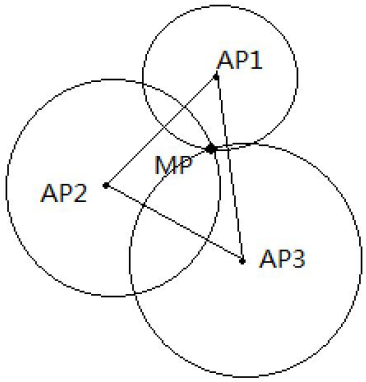

Figure 2.1: Principle of ToA -based positioning.

Moreover, it should be noted that despite the ToA-based positioning approach is with simple operation, and needs no complex transmitting and receiving equipment, it still faces some challenges, such as low positioning accuracy, high positioning error, and strict requirement time synchronization for the transmitter and receiver.

2.2.2 TDoA-based indoor positioning

In the Time Difference of Arrival (TDOA) scheme, the node to be located directly sends two different signals to the reference node that has been set in advance. Compared with ToA-based positioning scheme, there is no need to perform strict time synchro nization on the transmitting and receiving end, and only the arrival time to the reference node for the two different signals needs to be measured. At this time, the distance between the transmitter and the receiver can be obtained by multiplying the half difference time and the signal's propagation speed. Fig. 2.2 depicts the principle of TDoA-based positioning technology. As shown in Fig. 2.2, MP indicates the object's position to be estimated. AP_1, AP_2 and AP_3 indicate three access points with known position information. Hence, the three access points can make up a hyperbolic line with two random access points as focus. Since MP must be inside a triangle formed by AP_1, AP_2 and AP_3, the position of MP can be derived by solving the intersection of the three hyperbolic lines.

In addition, the advantage of TDoA -based positioning is that there is no need for strict time synchronization, and the hardware equipment at the receiving end is simple. However, its limitation is that the transmitter needs to be able to send two different signals.

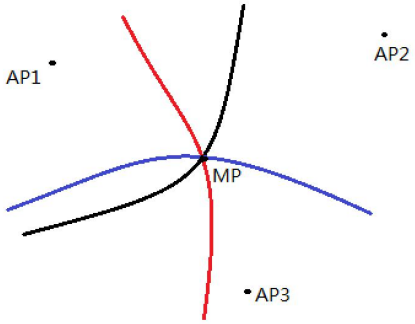

Figure 2.2: Principle of TDoA -based positioning.

2.2.3 CSI-based indoor positioning

Due to the time variability of the wireless channel, the multipath effect will also change with time going by. To depict the characteristic of the wireless channel model, indicators including the time delay, frequency attenuation, and Doppler frequency shift generated on all paths, are adopted to establish the wireless channel model, which is further represented by the Channel Impulse Response (CIR) function. When the spectrum of the received and transmitted signals is known, the Channel Frequency Response (CFR) which reflects the multipath characteristics of the channel can be calculated. Then, based on the Inverse Fourier Transform (IFT) approach, the CIR can be calculated, where Channel State Information (CSI) is the sample version of CIR/CFR under one specific transmission protocol.

To be specific, in the CSI-based indoor positioning scene, according to the signal attenuation during propagation, the channel model for signal propagation can be established. After combining the environmental factors in different scenarios, the position information of the target point can be estimated through related operations. In summary, the advantage of CSI-based indoor positioning is that the multipath propagation of signals can be better solved and characterized. However, the complex mathematical model and workload of signal processing also hinder the implement of this scheme.

2.3 System model and problem formulation

2.3.1 RSS-based positioning model

In the RSS-based positioning scheme, the premise is to establish the fingerprinting database of the WiFi signal, where the RSS value can be related to the geometry position. Then, for the target object to be located, we only need to measure the RSS value, and compare such value with the fingerprinting database to estimate the position by the matching algorithm. Specifically, in the indoor environment, the sum of multipath signals can be expressed as:

$$V = \sum_{i=1}^{N} |V_i| \, e^{-j\theta_i t} \tag{2.2}$$

Where $|V_i|$ and $|\theta_i|$ represent the amplitude and phase of the i^{th} path's signal, and N is the total number of paths. At this time, the RSS value can be calculated as:

$$RSSI = 20 \log_{10} |V| \tag{2.3}$$

Without loss of generality, on the one hand, when the target object is within the plane of two dimensions, at least three access points, i.e., anchor points, with known position need to be placed in advance. On the other hand, if the target locates at the space of three dimensions, there are at least four access points with known position deployed in the indoor environment [25].

2.3.2 Kalman Filtering Algorithm

In the wireless communication system, the Kalman filtering algorithm can reduce the errors resulted from the environment noise. As far as the Kalman filtering algorithm is concerned, based on the measured value in the current data and the predicted value and error at the previous moment, it can calculate the current optimal amount, and predict the data value at the next moment. It should be noted that the error is included in the calculation process, which is specifically divided into prediction error and measurement error, i.e., noise. Besides, the errors exist independently and are not always affected by data measurement. To be specific, the general form of the Kalman filtering algorithm is detailed as the following five steps.

Step1: One step prediction equation of state:

$$\hat{x}_k^- = A\hat{x}_{k-1} + Bu_{k-1} \tag{2.4}$$

Step2: One-step prediction of mean square error:

$$P_k^- = AP_{k-1}A^T + Q \tag{2.5}$$

Step3: Filter gain equation (weight):

$$H_k = \frac{P_k^- H^T}{HP_k^- H^T + R} \tag{2.6}$$

Step4: Filter estimation equation (optimal value):

$$\hat{x}_k = \hat{x}_k^- + K_k \left(\mathrm{Z}_k - H\hat{x}_k^- \right) \tag{2.7}$$

Step5: Filter the mean square error update matrix:

$$P_k = \left(\mathrm{I} - \mathrm{K}_k \mathrm{H} \right) P_k^- \tag{2.8}$$

where $\hat{x}_{k-1}$, $\hat{x}_k$ respectively represent the posterior state estimates at time $k-1$ and k; $\hat{x}_k^-$ represent the prior state estimates at time k; P_k represent the posterior estimate covariance at k; P_k^- represent the prior estimate covariance at k; H is the transformation matrix from state variables to observations; Z_k represents the measured value; K_k represents the filter gain matrix; A represents the state transition matrix; Q represents the covariance of the system excitation process; R

represents the measurement noise covariance, and B represents the matrix that converts the input to the state.

2.3.3 Problem formulation

Based on the above established models and analysis, in the indoor environment, the goal of this paper is to minimize the positioning error with less implementation cost, which is based on the RSS value of the WiFi signal, and maintain the communication function according to the WiFi signal's CSI information at the same time.

2.4 Empirical model-based indoor positioning with WiFi

2.4.1 Basic idea

In this section, to realize the indoor positioning with WiFi signal's RSS value, one empirical model-based positioning scheme is put forward. Specifically, we firstly determine the indoor environment for RSS data collection. Then, after Gaussian filtering and Kalman filtering, linear coding of the original data is adopted to improve the reliability of the data. Finally, we use the processed RSS data to construct the empirical model, where the least square method is used to obtain the optimal positioning model.

2.4.2 Data collection

To meet the needs of minimum positioning accuracy, the indoor environment should be divided accordingly, where the size of the grid points can directly influence the positioning accuracy. As is known that two-dimensional plane positioning technology requires three access nodes, and three border nodes are selected as access nodes in the grid. At each grid point, we measure and record the grid's RSS values, which are from three access nodes in turn. Each grid point is measured 100 times to eliminate the influence of measurement errors on the data.

2.4.3 Data processing

There are two main steps in the data processing stage. To be specific, at first, the collected RSS data is processed with the Gaussian and Kalman double filtering operations. Then, we perform linear coding operation on the filtered data, by which the influence brought by the equipment difference can be eliminated.

2.4.4 Curve fitting-based empirical model

In this subsection, the curve fitting-based empirical model is adopted to realize the RSS-based indoor positioning. In general, three major operations are performed by the following steps:

Step1: Construct appropriate empirical models (i.e., Gaussian fit, polynomial fit, and double exponential fit);

Step2: Adopt the least squares to perform the fit test;

Step3: Add weight to the established empirical model, which can improve the reliability of the data.

Mathematically, the above illustrations can be further expressed as the following four steps:

Step1: Deploy M access nodes in the indoor environment, and divide the measurement site into N grid points. Hence, there are M sets of raw RSS data, i.e.,

$$A = \begin{pmatrix} A_1 \\ \vdots \\ A_M \end{pmatrix} = \begin{pmatrix} (\mathrm{x}_1, \mathrm{y}_1, \mathrm{RSSA}_1(1)) & \cdots & (\mathrm{x}_N, \mathrm{y}_N, \mathrm{RSSA}_N(N)) \\ \vdots & \ddots & \vdots \\ (\mathrm{x}_1, \mathrm{y}_1, \mathrm{RSSA}_M(1)) & \cdots & (\mathrm{x}_N, \mathrm{y}_N, \mathrm{RSSA}_M(N)) \end{pmatrix} \tag{2.9}$$

Step2: After performing the double filtering, linear coding and other signal processing operations, the RSS data can be denoted as:

$$A' = F \cdots C \cdots A \tag{2.10}$$

Where F is the filtering process, and C represents the linear encoding process.

Step3: Establish the relationship between the processed RSS data and the geometry position of the measured grid points, which is expressed as:

$$Y = \begin{pmatrix} \mathrm{RSSA}_1 \\ \vdots \\ \mathrm{RSSA}_M \end{pmatrix} = g \begin{pmatrix} (\mathrm{x}_1, \mathrm{y}_1) & \cdots & (\mathrm{x}_N, \mathrm{y}_N) \\ \vdots & \ddots & \vdots \\ (\mathrm{x}_1, \mathrm{y}_1) & \cdots & (\mathrm{x}_N, \mathrm{y}_N) \end{pmatrix} \tag{2.11}$$

Among them, g represents the mapping relationship of functions.

Step4: Determine the weighting coefficient of each RSS function, mathematically,

$$(\mathrm{x}_i, \mathrm{y}_i) = \mathrm{K} \cdot \mathrm{g}^{-1}[\mathrm{Y}] \tag{2.12}$$

where K is a matrix of weighting coefficients, and

$$\begin{aligned} K &= \begin{pmatrix} k_1 \\ \vdots \\ k_m \end{pmatrix} \\ k_i &= \frac{RSSi(i)}{\sum_{j=1}^{n} RSSj(j)} \end{aligned} \tag{2.13}$$

2.5 Theoretical analysis for WiFi-based indoor communication

In this section, we use theoretical analysis to derive the mathematical expression of the indoor wireless channel transmission function. Besides, we also optimize the derived transmission function by considering the noise and inter-channel effects in theory. At last, a more applicable transmission function model is derived

in the mathematical form.

2.5.1 Wireless channel modeling in SISO scenario

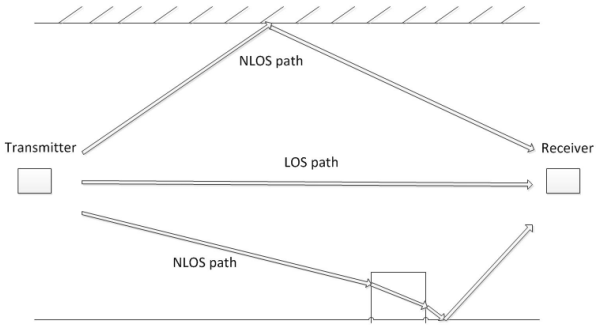

Figure 2.3: Wireless channel model of SISO scenario.

As shown in Fig. 2.3, the wireless channel model of SISO scenario is presented. When there are n paths in the wireless channel, the expression of the CIR function $h(t)$ can be further written as:

$$\begin{aligned} h(\mathrm{t}) &= [\alpha_1, \alpha_2, \alpha_3 \cdots \alpha_n] \cdot \begin{pmatrix} \delta(\mathrm{t}-\tau_1) & & 0 \\ & \ddots & \\ 0 & & \delta(\mathrm{t}-\tau_n) \end{pmatrix} \\ &\cdot \left[\mathrm{e}^{-j2\pi f_{q_q} t}, \mathrm{e}^{-j2\pi f_{q_d} t}, \mathrm{e}^{-j2\pi f_{\phi_j t}}, \cdots \mathrm{e}^{-j2\pi f_{\phi_n t}} \right] \\ &= \alpha \cdot \delta \cdot f_d \end{aligned} \tag{2.14}$$

where the matrix α represents the fading, the matrix δ means the delay, and the matrix f_d represents the Doppler frequency shift generated on the propagation path.

2.5.2 Wireless channel modeling in OFDM-based MIMO scenario

Multiple orthogonal subcarrier signals are used in the Orthogonal Frequency Division Multiplexing (OFDM) technology, where the data is divided into several sub-data streams, thereby reducing the transmission rate of the sub-data streams. Then, the divided data is utilized to modulate several carriers respectively, which is essentially a frequency division multiplexing technology. In summary, OFDM can effectively resist the effects of multipath.

Assume that the input signal is $x(t)$, after analog-to-digital conversion, $x(n)$ is obtained. Specifically, when the number of subcarriers is N, after serial-to-parallel transformation, a set of sequences with the same number of subcarriers (N) is obtained, i.e., $x1(n), x2(n), x3(n)...xN(n)$. After the carrier modulation operation (which is performed by IFFT in OFDM), the data is sent to the wireless channel. Since there are many multipaths of the wireless channel, M is selected as the main object of the channel modeling (the energy proportion of these M paths should reach more than 80% of the total energy). At this time, the attenuate and

delay of OFDM symbols is performed by the M paths the accordingly. Finally, the signal is sampled at the receiving end to obtain various sets of CSI values, where CSI values contains the corresponding phase and amplitude information of each subcarrier. Mathematically,

$$x(\mathrm{t}) \overset{A/D}{\rightarrow} \begin{Bmatrix} x_1(\mathrm{n}) \\ x_2(\mathrm{n}) \\ x_3(\mathrm{n}) \\ \vdots \\ x_N(\mathrm{n}) \end{Bmatrix} \overset{\text{wireless channel}}{\rightarrow} \begin{Bmatrix} \mathrm{CSI}_1 : \alpha_1 e^{j2\pi(\mathrm{f}_1+\tau_1)}, \alpha_2 e^{j2\pi(\mathrm{f}_1+\tau_2)}, \cdots \alpha_M e^{j2\pi(\mathrm{f}_1+\tau_M)} \\ \mathrm{CSI}_2 : \alpha_1 e^{j2\pi(\mathrm{f}_2+\tau_1)}, \alpha_2 e^{j2\pi(f_2+\tau_2)}, \cdots \alpha_M e^{j2\pi(f_2+\tau_M)} \\ \mathrm{CSI}_3 : \alpha_1 e^{j2\pi(\mathrm{f}_3+\tau_1)}, \alpha_2 e^{j2\pi(f_3+\tau_2)}, \cdots \alpha_M e^{j2\pi(\mathrm{f}_3+\tau_M)} \\ \vdots \\ \mathrm{CSI}_M : \alpha_1 e^{j2\pi(\mathrm{f}_M+\tau_1)}, \alpha_2 e^{j2\pi(\mathrm{f}_M+\tau_2)}, \cdots \alpha_M e^{j2\pi(\mathrm{f}_M+\tau_M)} \end{Bmatrix} \tag{2.15}$$

In addition, the above process can be further expressed as:

$$[X \cdot S] * [\alpha \cdot H] = Y \tag{2.16}$$

where the * sign indicates a convolution operation, X represents an original signal, S means a serial-to-parallel transformation, α is fading on each path, and system transfer function is denoted by H.

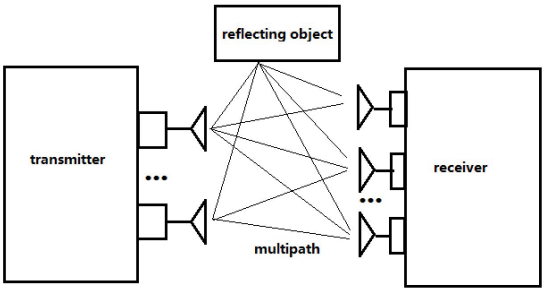

Figure 2.4: Wireless channel model of MIMO.

As shown in Fig. 2.4, in a MIMO system. When the the i^{th} antenna in the transmitting end is selected to send the data, and the the j^{th} antenna is in charge of receiving signals in the receiving end. At this time, the state of sending and receiving can be viewed as the process of using OFDM technology under the SISO condition. When p transmitting antennas and q receiving antennas are adopted, the expression of the sending signal is:

$$\mathrm{X(t)} = \left[\mathrm{x}_1^T(\mathrm{t}), \mathrm{x}_2^T(\mathrm{t}), \mathrm{x}_3^T(\mathrm{t}) \cdots \mathrm{x}_p^T(\mathrm{t})\right]^T \tag{2.17}$$

The expression of the received signal is:

$$\mathrm{Y(t)} = \left[y_1^T(\mathrm{t}), y_2^T(\mathrm{t}), y_3^T(\mathrm{t}) \cdots y_q^T(\mathrm{t})\right]^T \tag{2.18}$$

Hence, the CSI at this time can be expressed as follows:

$$\mathrm{Y(t)} = \left[y_1^T(\mathrm{t}), y_2^T(\mathrm{t}), y_3^T(\mathrm{t}) \cdots y_q^T(\mathrm{t})\right]^T \tag{2.19}$$

where h_{pq} is a complex number representing the amplitude and phase of the subcarriers in the antenna stream. Besides, the above process can also be expressed in the matrix form as:

$$H\left(f_k\right)=\begin{pmatrix} h_{11} & h_{12}\cdots & h_{1q} \\ h_{21} & h_{22}\cdots & h_{2q} \\ \cdots & \cdots\cdots & \cdots \\ h_{p1} & h_{p2} & h_{pq} \end{pmatrix} \tag{2.20}$$

In summary, when that the i^{th} antenna transmits data and the j^{th} antenna receives information. After the above analysis, the system transfer functions of LOS and several other non-LOS paths can be obtained. Under the premise of transmitting signals at a known transmitting end, by performing convolving the transmitting signal with the transmission function, the received signal can be obtained.

2.6 Evaluation results and performance analysis

2.6.1 Experiment settings

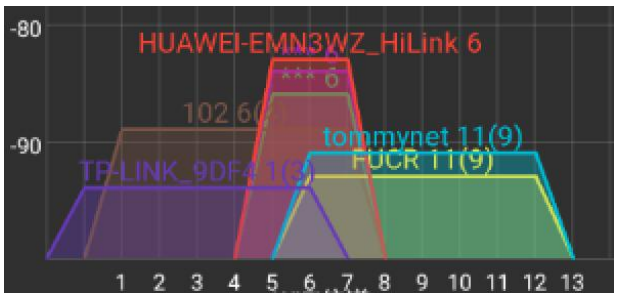

Figure 2.5: The interface of different signal RSS value.

The RSS-based indoor positioning experiment is conducted in the aisle, third floor, Research Building, University of Aizu. Besides, the experimental mobile device is the smartphone with android [26]. Fig. 2.5 shows the measurement of different signal's RSS values, where the interface is the screenshot of smartphone application named WiFi ANALYSIS ASSISTANT, and the deployment of the access points is shown in Fig. 2.6

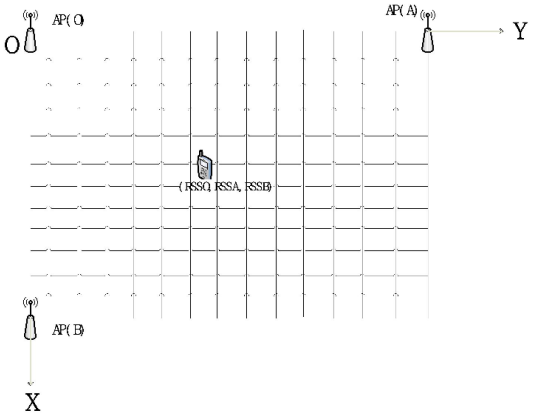

Figure 2.6: The deployment of the access points.

2.6.2 Indoor positioning performance evaluation with numerical results

After Gaussian filtering and Kalman filtering processing, the position of each point in the aisle is represented by two-dimensional coordinates, and the best RSS value corresponding to each point is obtained.

Table 2.2: RSS value of different position.

(x, y) (m)	(RSSO, RSSA,RSSB) (-dBm)	(X, Y) (m)	(RSSO, RSSA,RSSB) (-dBm)
(0.00, 0.00)	(-34, -74, -82)	(0.86, 0.00)	(-66, -76, -63)
(0.00, 0.60)	(-57, -72, -79)	(0.86, 0.60)	(-67, -71, -65)
(0.00, 1.20)	(-69, 70, -78)	(0.86, 1.20)	(-74, -70, -66)
(0.00, 1.80)	(-78, -62, -75)	(0.86, 1.80)	(-76, -66, -68)
(0.00, 2.40)	(-81, -25, -72)	(0.86, 2.40)	(-77, -64, -73)
(0.43, 0.00)	(-61, -73, -77)	(1.29, 0.00)	(-70, -75, -35)
(0.43, 0.60)	(-63, -68, -76)	(1.29, 0.60)	(-71, -74, -48)
(0.43, 1.20)	(-65, -75, -75)	(1.29, 1.20)	(-72, -78, -70)
(0.43, 1.80)	(-73, -69, -73)	(1.29, 1.80)	(-75, -77, -66)
(0.43, 2.40)	(-71, -58, -70)	(1.29, 2.40)	(-80, -85, -77)

At this time, after adopting the curve fitting-based approach, we can draw the three-dimensional images of the coordinates and the RSS values of each measured point separately. For ease of presentation, we have taken the absolute value of the signal strength.

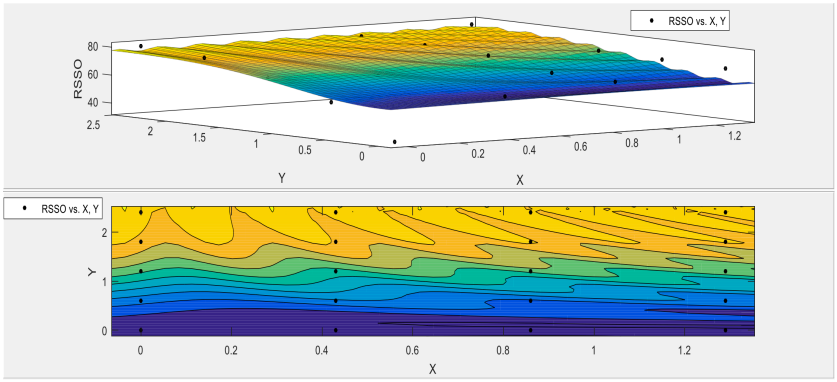

Figure 2.7: Relation between RSSO and position.

It can be seen from Fig. 2.7, Fig. 2.8 and Fig. 2.9 that after the fitting process, the three graphs respectively represent the functions between the RSS of access point O, RSS of access point A, RSS of access point B, and the geometry coordinates (x, y) of the plane. To be specific, the upper half of the Figure shows the three-dimensional relationship, and the lower half shows the top view. From these results, the closer the signal access points are, the denser it is, which evaluates the correctness of the proposal.

In the judgment process, the weighted fusion method in data fusion is adopted for the confidence of the three access points' RSS values, and the weights of the three points are set as follows:

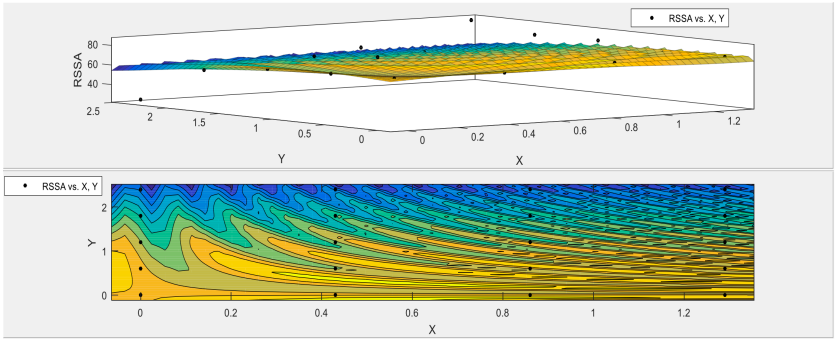

Figure 2.8: Relation between RSSA and position.

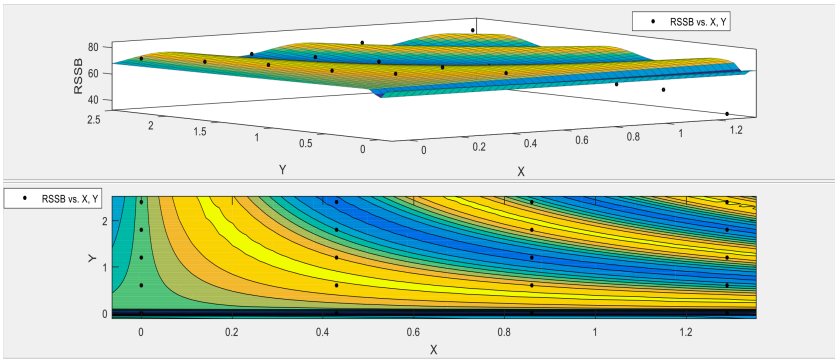

Figure 2.9: Relation between RSSB and position.

$$\left(\frac{RSSO(\mathrm{O})}{RSSO(\mathrm{O})+\mathrm{RSSA(A)}+\mathrm{RSSB(B)}}, \frac{\mathrm{RSSA(A)}}{RSSO(\mathrm{O})+\mathrm{RSSA(A)}+\mathrm{RSSB(B)}}, \frac{RSSB(\ \mathrm{B})}{RO(\mathrm{O})+\mathrm{RSSA(A)}+\mathrm{RSSB}}\right.$$
$$= (\mathrm{K}_1,\ \mathrm{K}_2,\ \mathrm{K}_3) = \left(\frac{34}{94}, \frac{25}{94}, \frac{35}{94}\right) = (0.36, 0.27, 0.37) \tag{2.21}$$

where the RSS values of the $RSSO(O), RSSA(A), RSSB(B)$ corresponds to the three access points measured at three access points of O, A, and B in order.

In order to prove the effectiveness of the proposed scheme, we use the positioning error indicator to make comparison experiment with the traditional $WKNN$ algorithm and the traditional joint probability algorithm here. The expression of the positioning error is:

$$\text{pos err} = \sqrt{(\mathrm{x}-\mathrm{x}_0)^2 + (y-y_0)^2} \tag{2.22}$$

where (x, y) represents the estimated coordinates of the object, and (x_0, y_0) represents the actual coordinates of the object.

After estimating the position of the object 100 times, the accuracy comparison results of several traditional positioning algorithms are as follows:

1. The positioning error of the traditional WKNN algorithm is 0.37m.
2. The positioning error of the traditional joint probability algorithm is 0.53m.
3. The positioning error of the WKNN algorithm based on the joint probability class is 0.48m.
4. The positioning error of our algorithm is 0.25m.

2.6.3 Indoor communication function verification in theory

In this subsection, we verify the indoor communication function in theory. At first, the number of multipath channels is set as 6, the modulation method is BPSK modulation, and the ambient noise is additive white Gaussian noise. The detailed derivation process is listed as following steps.

Step1: The analog signal after digital-to-analog conversion can be transformed into signal X, which is denoted as:

$$\mathrm{X} = \begin{pmatrix} a_1 & \cdots & f_1 \\ \vdots & \ddots & \vdots \\ a_6 & \cdots & f_6 \end{pmatrix} \tag{2.23}$$

Step 2: After BPSK modulation, the signal can be further expressed as:

$$X_M = \begin{pmatrix} a_1' & \cdots & f_1' \\ \vdots & \ddots & \vdots \\ a_6' & \cdots & f_6' \end{pmatrix} \tag{2.24}$$

Step 3: When the data is transmitted through wireless multipath channel, it can be denoted as:

$$C = (\mathrm{CSI}_1, \cdots CS\mathrm{I}_6)^T = \begin{pmatrix} a_1' \cdot m_1 \cdot e^{jwt_1} & \ldots & a_6' \cdot m_6 \cdot e^{jwt_1} \\ \vdots & \ddots & \vdots \\ f_1' \cdot m_1 \cdot e^{jwt_1} & \ldots & f_6' \cdot m_6 \cdot e^{jwt_1} \end{pmatrix} \tag{2.25}$$

where the model of the wireless multipath channel is:

$$(H_1 \cdots H_6) = \left(\mathrm{m}_1 \cdot \mathrm{e}^{jwt_1} \cdots \mathrm{m}_6 \cdot \mathrm{e}^{jwt_6}\right) \tag{2.26}$$

$$h(\mathrm{t}) = \sum_{i=1}^{6} m_i \delta\left(\mathrm{t} - \mathrm{t}_i\right) \Rightarrow \mathrm{H(w)} = \sum_{i=1}^{6} m_i e^{jwt_i} \tag{2.27}$$

Step4: Denote H as the channel matrix,

$$H = \begin{pmatrix} H_1 & & 0 \\ & \ddots & \\ 0 & & H_6 \end{pmatrix} \tag{2.28}$$

Then, we have

$$C^T = X_M \cdot H \tag{2.29}$$

which can also be expressed as:

$$H = \left[\mathrm{X}_M\right]^{-1} \cdot C^T \tag{2.30}$$

Based on Equation 28, the multipath transmission function in the wireless channel can be obtained. In addition, under the AWGN conditions, the coefficient matrix K is introduced to improve the accuracy and reliability of the transmission

function. Specifically, the effect of introducing the coefficient matrix K mainly focuses on twofold: 1) Reduce the effect on the system transfer function after addictive Gaussian white noise; 2) Reduce the mutual influence between adjacent channels. At this time, denote the coefficient matrix K as:

$$K = \begin{pmatrix} k_{11} & \cdots & k_{16} \\ \vdots & \ddots & \vdots \\ k_{61} & \cdots & k_{66} \end{pmatrix} \tag{2.31}$$

When taking the addictive noise and the influence between adjacent channels into consideration, X_M becomes X'_M, mathematically,

$$X'_M - X_M = \begin{pmatrix} \sigma_{a1} & \cdots & \sigma_{f1} \\ \vdots & \ddots & \vdots \\ \sigma_{a6} & \cdots & \sigma_{f6} \end{pmatrix} \tag{2.32}$$

Hence, the following Equation holds on:

$$\begin{cases} X_M \cdot H = C^T \\ X'_M \cdot K \cdot H = C'^T \end{cases} \tag{2.33}$$

Next, we can use the minimum mean square error criterion to calculate the coefficient matrix K, and figure out K to minimize the following equation,

$$\begin{aligned} &\left|C'^T - C^T\right|^2 = \left|X'_M \cdot K \cdot H - X_M \cdot H\right|^2 \\ &= \left|X'_M \cdot K - X_M\right|^2 \cdot |H|^2 \\ &\Leftrightarrow \left| \begin{pmatrix} k_{11} & \cdots & k_{16} \\ \vdots & \ddots & \vdots \\ k_{61} & \cdots & k_{66} \end{pmatrix} \cdot \begin{pmatrix} a'_1 + \sigma_{a1} & \cdots & f'_1 + \sigma_{f1} \\ \vdots & \ddots & \vdots \\ a'_6 + \sigma_{a6} & \cdots & f'_6 + \sigma_{f6} \end{pmatrix} - \begin{pmatrix} a'_1 & \cdots & f'_1 \\ \vdots & \ddots & \vdots \\ a'_6 & \cdots & f'_6 \end{pmatrix} \right| \\ &= \left| \sum_{i,j=1}^{6} K_{ij} \cdot \left(\sum_{A'=\{\mathrm{a}'\ldots\mathrm{f}\}}^{6} A'_i + \sigma_{Ai} \right) - \sum_{A'=\{\mathrm{a}'\cdots\mathrm{f}\}}^{6} A'_i \right|^2 \end{aligned}$$

At last, the transmission function $\widehat{H}$, which represents the communication function of the wireless communication system, can be determined as:

$$\hat{H} = K \cdot H = K \cdot X_M^{-1} \cdot C^T \tag{2.34}$$

2.7 Conclusion and future work

The method for realizing indoor positioning and communication based on WiFi signals is of practical significance, and it is not difficult to implement and the cost is low. This paper proposes a new algorithm for indoor target positioning and communication integration based on WiFi signals. The RSS and CSI values in the WiFi signal are used to achieve indoor target positioning respectively, and the derived indoor wireless channel system transfer function is used to achieve the purpose of communication. In the positioning part based on the RSS value, the accuracy of the algorithm can reach 0.25m, which can meet the indoor positioning

requirements under certain conditions. In the communication part based on the CSI value, the transmission function of the indoor wireless channel is creatively described using the CSI value. The transmission function of the system is optimized under the conditions of noise and interference between adjacent channels. Finally, the goal of integration of positioning and communication based on WiFi signal level was achieved for the first time. In the next work, we need to further improve this algorithm, taking into account factors such as the movement of people indoors, the location of access points, and the transmission power of WiFi signals, so that our algorithm is more accurate, and the model we build is more complete to meet the characteristics of indoor complex wireless channel environment.

Chapter 3

Device-Free Localization via Sparse Coding with Log-Regularizer

3.1 Introduction

Wireless localization has been acknowledged as a critically important element of smart city. Many current localization techniques, e.g., global positioning system (GPS) [27] or radio frequency identification (RFID) [28], are device-based which means the target must be equipped with an electronic device (e.g., smart phone or tag). However, for many practical applications, such as intruder detection/tracking in security safeguards, aging monitoring at a smart home, patient tracking in a hospital, etc., the target may not expect to be equipped with extra devices [29].

Therefore, device-free localization (DFL) [30], as an emerging technology, has attracted extensive interest recent years because it locates targets who do not equip with any attached devices in wireless sensor networks [31, 32]. As shown in Fig. 3.1, in the Internet-of-Things (IoT) [33–35] baesd DFL system, wireless sensors, termed as anchor points (AP), are used to collect location-data by transmitting and receiving signals collaboratively. These transmitting-receiving correspondences, i.e., signal patterns induced by the targets, are different when the target appears at different locations. Therefore, the target's location can be known by analyzing the variations of radio frequency (RF) signals.

Since sensors generate the location-data with a pattern, i.e. feature, which is specific according to target's location, the sensing data with pattern information can be collected for location estimation. Thus, if the monitoring area is divided into a number of grids, each grid can be viewed as a potential class. From this point of view, many previous studies report that DFL problem can be transformed into a classification problem. The localization problem is consequently solved by many popular classification methods, for example, deep neural network (DNN) with auto-encoder [36], convolutional neural network (CNN) [29] and so on.

For such various classification methods, sparse coding [37] is famous for many distinctive advantages, e.g., simple decision rule, high accuracy and high efficiency in DFL field. Particularly, since the number of targets is generally far smaller than the grid number of detection area, localization problem can be further converted to a sparse-representation-classification (SRC) problem that can be effectively solved

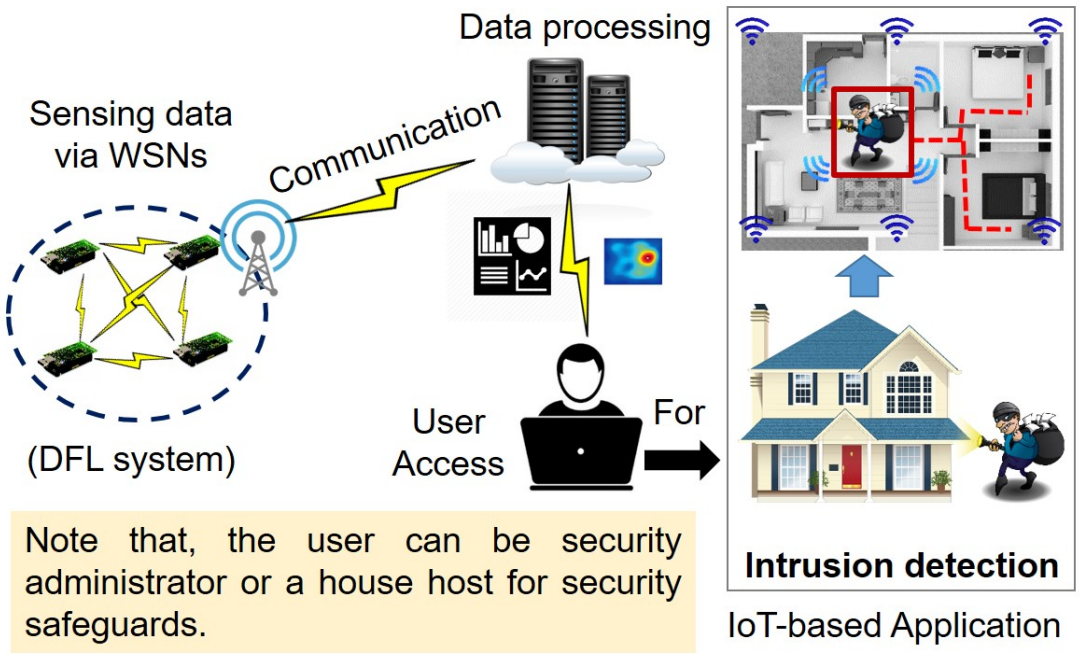

Figure 3.1: Illustration of a device-free localization (DFL) system applied to intrusion detection and tracking in security safeguard.

by sparse coding algorithm [38, 39].

It is worth noting that, for an SRC problem, the objective function usually consists of loss term and regularization term. Employing different regularization terms lead to different sparse-coding algorithms. Among those regularizers [40–42], the most famous ones are l_0 norm and l_1 norm which have been popularly adopted in the DFL field [37,38,43]. Generally, a (sparse) solution can be obtained by executing sparse-coding algorithm. Since the element index of solution are associated with the reference-point (RP) ID of DFL area, the location of the target is estimated by selecting the maximum element-value of a sparse solution when l_0 norm or l_1 norm is applied.

For the localization experiments in most of existing studies, the location-based signals are usually collected in a relatively clean and static experimental environment [1]. This leads their methods to achieving an accurate localization result. However, in practical scenarios, the detection environment may be very challenging, due to the vibration of sensors caused by wind, electromagnetic interference caused by surrounding smart phone or other wireless devices, etc. These negative effects result in the DFL data being collected with a certain degree of noise. This means DFL data is possible to be polluted, which is a serious negative condition for locating targets. In addition, for the privacy-preservation need, a common method is adding Gaussian noise in the original DFL data to keep network privacy from stealing by attackers. Thus, a robust algorithm is significant for locating the target in extreme environments or emergency scenarios.

Hence, to solve the aforementioned DFL problems, in this paper, we exploit a new log-regularizer in the objective function for classification. With taking the distinctive ability of log-regularizer to measure sparsity, the proposed approach is expected to achieve an accurate localization process with robust performance in the challenging environments. In addition, the objective function is not straight-

forwardly solvable because the log-regularizer is non-differentiable in some places. For overcoming this challenge, we exploit the proximal operator method to transform the non-smooth optimization problem, and then solve it by our proposed algorithm. Finally, through the proposed sparse coding with log-regularizer (SC-LR) algorithm, a sparse solution can be obtained for locating the target, which is expected to achieve more accurate localization results and a robust localization performance for DFL.

The major contributions of this article are summarized as follows:

- We exploit the log-regularizer to extend the applications of sparse-representation-based frameworks for DFL.
- We propose an accurate and robust DFL algorithm. Particularly, we exploit the effective optimization method with the proximal operator by transforming the original objective function.
- we validate the performance of the proposed approach on the real-world dataset of outdoor DFL, especially in severe noisy conditions.

The remainder of this paper is organized as follows. Section 3.2 introduces the system model and problem formulation. Section 3.3 introduce the objective function and the proposed algorithm. Section 3.4 conducts the performance evaluation. Finally, Section 3.5 shows the conclusions of this study.

3.2 Problem Formulation

3.2.1 The description of DFL problem

As shown in Fig. 3.2, a number of wireless devices is deployed around the DFL area. These wireless devices are normally called anchor points (APs), which can communicate with each other. Additionally, N is defined as the number of APs in the DFL system. Here, when there is no target in the DFL area, let $R_{i,j}^{\text{vacant}}$ denote the measurement of received signal strength (RSS) that is transmitted from the j-th AP to the i-th AP. $R_{i,j}^{\text{target}}$ denotes the measurement of RSS collected when there exit a target. Then, let $\Delta R_{i,j}$ denote the measurement variation between $R_{i,j}^{\text{target}}$ and $R_{i,j}^{\text{vacant}}$ as

$$\Delta R_{i,j} = R_{i,j}^{\text{target}} - R_{i,j}^{\text{vacant}} \tag{3.1}$$

Then an RSS matrix $\Delta \boldsymbol{R}$, considering all D×D pairs, can be established as follows:

$$\Delta \boldsymbol{R} = \begin{bmatrix} \Delta R_{1,1} & \Delta R_{1,2} & \cdots & \Delta R_{1,N} \\ \Delta R_{2,1} & \Delta R_{2,2} & \cdots & \Delta R_{2,N} \\ \vdots & \vdots & \ddots & \vdots \\ \Delta R_{N,1} & \Delta R_{N,2} & \cdots & \Delta R_{N,N} \end{bmatrix} \tag{3.2}$$

As shown in Fig. 3.2, the target absorbs and scatters some of the transmitted signals in the DFL area. When the target is in different locations, RSS measurements of the affected links are different. Therefore, the measurement variation could be used to estimate the target's location.

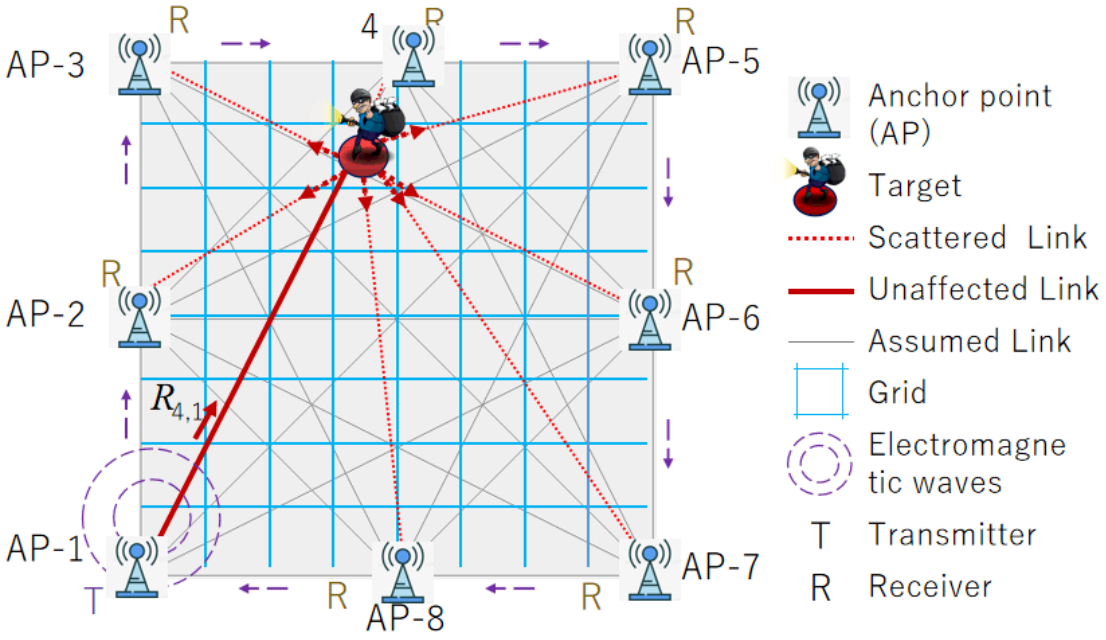

Figure 3.2: Illustration of a device-free localization (DFL) system model.

3.2.2 Sparse representation model

3.2.2.1 Dataset construction

There are two steps for dataset construction:

Step 1 is for building up a sensing matrix, or called *dictionary*. Discrete the DFL area into many small grids, as shown in Fig. 3.2, assuming the total number of them is C. Each grid is regarded as one location at which we perform a number of trials. Therefore, all the potential localization are divided into C classes in this DFL problem. For each class $c = 1, 2, \cdots, C$, we perform experiments of $l = 1, \cdots, L$ trials with a target at each grid. After data collection, for each trial, we can get an matrix data shown as $\Delta \boldsymbol{R}_{cl} \in \mathbb{R}^{N \times N}$. Then convert the matrix $\Delta \boldsymbol{R}_{cl}$ to a variation vector $\boldsymbol{d}_{cl}$ by merging all the columns into the vector. Finally, stacking all the variation vectors together, we can obtain the sensing matrix with location information for all grids and trials as $\boldsymbol{D} = [\boldsymbol{d}_{11}, \boldsymbol{d}_{12}, \cdots \boldsymbol{d}_{1L}, \cdots, \boldsymbol{d}_{c1}, \cdots, \boldsymbol{d}_{cL}, \cdots, \boldsymbol{d}_{C1}, \cdots, \boldsymbol{d}_{CL}]$. This sensing matrix $\boldsymbol{D}$ is normally termed as dictionary with a size of $m \times n$, where $m = N^2, n = CL$.

Step 2 is for processing the test signal. When a testing target is put into the DFL area, the same procedure is taken for processing the observation signal. we can obtain the vector of observation signal as $\mathbf{y} \in \boldsymbol{R}^m$.

3.2.2.2 Sparse representation of testing signal

According to the last part 3.2.2.1, in the testing step, when a target enters the DFL area, a (testing) observation signal $\boldsymbol{y}$ will be obtained. Suppose that the target is, approximately, at the p-th grid, it means that target belongs to the p-th class. If sufficient samples are given, i.e. conducting enough trials at the p-th grid in Step 1 of constructing dictionary, the testing signal $\boldsymbol{y}$ can be represented

with the corresponding sample-set of dictionary $\boldsymbol{D}$. The representation is given as follows:

$$\begin{aligned} \boldsymbol{y} &= \boldsymbol{D}\boldsymbol{\alpha} + \boldsymbol{e} \\ &= \sum_{c=1}^{C} \sum_{l=1}^{L} \boldsymbol{d}_{cl}\alpha_{cl} + \boldsymbol{e} \\ &\approx \sum_{l=1}^{L} \boldsymbol{d}_{pl}\alpha_{pl} \\ &\text{for } 1 < p < C, \end{aligned} \tag{3.3}$$

where $\boldsymbol{\alpha} = [0 \ \cdots \ \alpha_{p1} \cdots \alpha_{pL} \ \cdots \ 0]^T \in \mathbb{R}^n$ is a vector comprised of coefficients, $\alpha_{pj} \in \mathbf{R}$ (for $1 < j < L$) are the non-zero coefficients belonging to the p-th class and $\boldsymbol{e}$ indicates the noise.

In summary, due to the sparse nature of DFL that the number of targets' locations is far less than all grids of the monitoring area, the linear representation of observation signal $\boldsymbol{y}$ can be sparsely represented in terms of n basis samples of the dictionary $\boldsymbol{D}$. From this point of view, (3.3) becomes a sparse representation problem for target localization, where $\boldsymbol{\alpha}$ is corresponding to a sparse coefficient vector. In the vector of $\boldsymbol{\alpha}$, nonzero elements are associated to targets' locations. To make it more clear, we present the entire model in Fig. 3.3. It is worthy of note that one target may have several corresponding components in $\boldsymbol{\alpha}$.

3.3 Proposed Algorithms

According to the above description, if the sparse coefficient vector $\boldsymbol{\alpha}$ is obtained, the location of the target can be obtained. Hence, the DFL problem is transformed to computing the sparse vector. As mentioned previous, in practical applications, a robust DFL algorithm is necessary for working in the extreme environments. In this section, we introduce the proposed algorithm that it used to solve the DFL problem.

3.3.1 Sparse coding

Sparse coding is a process of computing the sparse solution based on the observation signal $\boldsymbol{y}$ and the pre-built dictionary $\boldsymbol{D}$. In practice, it is essential to employ a large number of trials to build the dictionary. Thereby, the total number of basis samples n is larger than m for the dictionary as shown in Fig. 3.3. The above mentioned condition leads to (3.3) a undetermined system, which means the solution is not unique and the problem is ill-posed.

However, by selecting the sparsest solution, the problem can be converted into well-posed one. We can find the sparsest solution by solving the optimization problem with a sparsity regularization.

3.3.2 objective function

For solving the DFL problem in challenging environment, in this article, we proposed a new sparsity regularizer and called it as log-regularizer. The objective

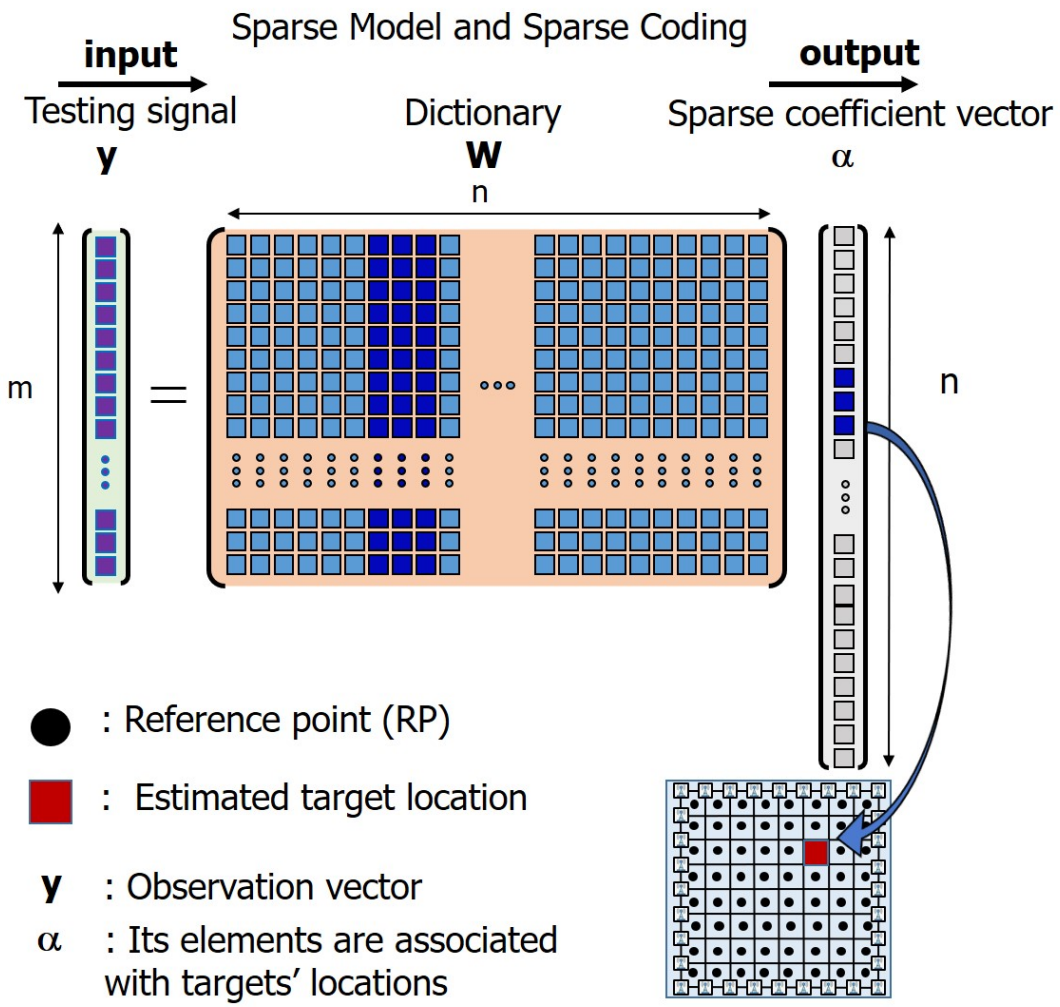

Figure 3.3: Illustration of the sparse model and the procedure of sparse coding for target localization.

function is given as follows:

$$J(\boldsymbol{\alpha}): \quad \boldsymbol{\alpha}^* = \underset{\boldsymbol{\alpha}}{\operatorname{argmin}} \frac{1}{2} \|\boldsymbol{y} - \boldsymbol{D}\boldsymbol{\alpha}\|_2^2 + \lambda \sum_i \log(1 + \xi|\alpha_i|) \tag{3.4}$$

where the first term $\|\cdot\|_2^2$ is a measure of fitting error between observation signal and estimated signal; the second term is sparsity regularizer; λ is a scalable parameter which trades off the fitting error and the sparsity; ξ is a scalable parameter about the regularizer.

3.3.3 Sparse coding via the proximal operator

Since (3.4) is a non-smooth optimization problem, sub-gradient method is normally applied. If let the derivative of (3.4) to zero, we get an $\boldsymbol{\alpha}^*$,

$$\boldsymbol{\alpha}^* = (\boldsymbol{D}^T\boldsymbol{D} + \lambda \frac{\partial(\|\boldsymbol{\alpha}\|_{2,1})}{\partial \boldsymbol{\alpha}})^{-1}\boldsymbol{D}^T\boldsymbol{y} \tag{3.5}$$

However, calculating (3.5) with sub-gradient method is not easy. The reason is, solving $(\boldsymbol{D}^T\boldsymbol{D})^{-1}$ will result in a high computational cost if dictionary $\boldsymbol{D}$ is with very large dimensions. Also, $(\boldsymbol{D}^T\boldsymbol{D})^{-1}$ may not be invertible.

In this section, to well solve this problem, we exploit the proximal operator method to search the sparse solution. Proximal operator is efficient for solving the non-smooth and non-differentiable optimization problem. If different regularization term is adopted in a objective function, there will be a corresponding proximal operator derived. Regarding the case of (3.4), a general formula is given as follows,

$$P(\boldsymbol{v}): \quad \underset{\boldsymbol{v}}{\operatorname{argmin}}\ \eta\|\boldsymbol{u}-\boldsymbol{v}\|_2^2+\gamma\sum_i \log(1+\xi|\nu_i|) \tag{3.6}$$

Coinciding with (3.6), we need make a modification to (4). Through a transformation, let us consider a simpler one than (3.4),

$$P(\boldsymbol{\alpha}): \quad \underset{\boldsymbol{\alpha}}{\operatorname{argmin}}\ \frac{\mu}{2}\|\boldsymbol{b}-\boldsymbol{\alpha}\|_2^2+\lambda\sum_i \log(1+\xi|\alpha_i|)+\ K \tag{3.7}$$

where the term K does not depend on $\boldsymbol{\alpha}$, it is processed as a constant; μ, as a scaling parameter, is fixed with a value larger than the largest eigenvalue of $(\boldsymbol{D}^T\boldsymbol{D})$, e.g., $1.02\times$ *the largest eigenvalue*; $\boldsymbol{b}$ is a intermediate variable that is given as follows,

$$\boldsymbol{b}=\boldsymbol{\alpha}^{(k)}+\frac{1}{\mu}\boldsymbol{D}^T(\boldsymbol{y}-\boldsymbol{D}\boldsymbol{\alpha}^{(k)}) \tag{3.8}$$

$$\begin{aligned}\boldsymbol{\alpha}^{(k+1)}&=\operatorname{prox}_{log}(\boldsymbol{b})\\&=\operatorname{prox}_{log}(\boldsymbol{\alpha}^{(k)}+\frac{1}{\mu}\boldsymbol{D}^T(\boldsymbol{y}-\boldsymbol{D}\boldsymbol{\alpha}^{(k)}))\end{aligned} \tag{3.9}$$

where $\boldsymbol{\alpha}^{(0)}=\boldsymbol{0}$; $\operatorname{prox}_{log}(\cdot)$ is the proximal operator**,** corresponding to the log-regularizer, given by

$$\operatorname{prox}_{\|\cdot\|_{log}}(b_i)=\begin{cases}\dfrac{1}{2\xi}\left((\xi b_i+1)-\sqrt{(ab_i-1)^2-2\lambda\xi^2}\right), & b_i<-\dfrac{\lambda\xi}{2}\\[2ex] \dfrac{1}{2\xi}\left((\xi b_i-1)-\sqrt{(ab_i+1)^2-2\lambda\xi^2}\right), & b_i>\dfrac{\lambda\xi}{2}\\[2ex] 0, \text{otherwise}\end{cases} \tag{3.10}$$

where b_i is the i-th element of vector $\boldsymbol{b}$.

The optimization process mainly updates parameters via (3.8)-(3.10) at each iteration. Until reach the convergence or the stop rule is met, the optimal solution α^* is then fixed.

Further, we estimate target's locations according to the optimal sparse solution $\boldsymbol{\alpha}^*$. Since the elements of$\boldsymbol{\alpha}^*$ are associated with the reference grid of monitoring area, the related grid can be estimated as target's location. For example, for a monitoring area with the total C grids, the target is located at the φ-th grid,

Algorithm 1 Sparse Coding with Log-Regularizer (SC-LR)

Require: $\boldsymbol{y} \in \mathbb{R}^m$, $\boldsymbol{D} \in \mathbb{R}^{m \times n}$, μ, λ, $\boldsymbol{\alpha}_0 = \mathbf{0}$
Ensure: φ or $\{\varphi_1, \ldots, \varphi_S\}$
1: **for** $k = 0$ to maxiteration **do**
2: $\quad \boldsymbol{b} \leftarrow \boldsymbol{\alpha}^{(k)} + \frac{1}{\mu}\boldsymbol{D}^T(\boldsymbol{y} - \boldsymbol{D}\boldsymbol{\alpha}^{(k)})$
3: $\quad \boldsymbol{\alpha}^{(k+1)} \leftarrow \text{prox}_{\|\cdot\|_{log}}(\boldsymbol{b})$
4: $\quad$ Until convergence or reach the maxiteration number.
5: **end for**
6: $\boldsymbol{\alpha}^* \leftarrow \boldsymbol{\alpha}^{(k+1)}$
7: Target is located at the φ-th grid according to (3.11)
8: **Return** φ

where φ is given by

$$\varphi = \underset{\varphi}{\text{argmax}}\{\alpha^*_{11}, \cdots, \alpha^*_{\varphi i}, \cdots, \alpha^*_{CL}\} \tag{3.11}$$

Since the proposed algorithm is with the log-regularizer, it is named sparse coding with log-regularizer (SC-LR). The corresponding pseudo-code is shown in Algorithm 1.

3.4 Performance Evaluation

3.4.1 Experimental settings

We use a real-world dataset from the SPAN Lab of University of Utah [1]. As shown in Fig. 3.4, the experiment setup is as follows. The monitoring area is with a 21x21 foot square and is divided into 36 grids. 28 wireless (TelosB) sensor nodes are employed in this system and work in the 2.4 GHz frequency band. The interval is 3 feet between two neighbour nodes and all the nodes are placed at 3 feet off the ground.

The base station is refitted with a TelosB node which listens to the whole network traffic. It collects the real-time data from the other sensors and deliveries them to the computer by a USB port. At each grid, 30 RSS samples are collected with a very short time-interval.

In our following experiments, the samples collected at each grid are partitioned into two parts, of which 25 samples are for constructing dictionary while the others are used as test samples. The dimension dictionary is with 784× 900 while a test sample is with 784× 1. All the experiments are performed in MATLAB® R2019a and executed on a computer of Windows10 64-bit with 32GB RAM and Intel® Core™ i7 CPU.

3.4.2 Compared methods

To present the distinctive performance of the proposed scheme, several machine-learning methods that perform on the same dataset are compared in the following contents. Among these compared algorithms, Autoencoder (AE), deep CNN and

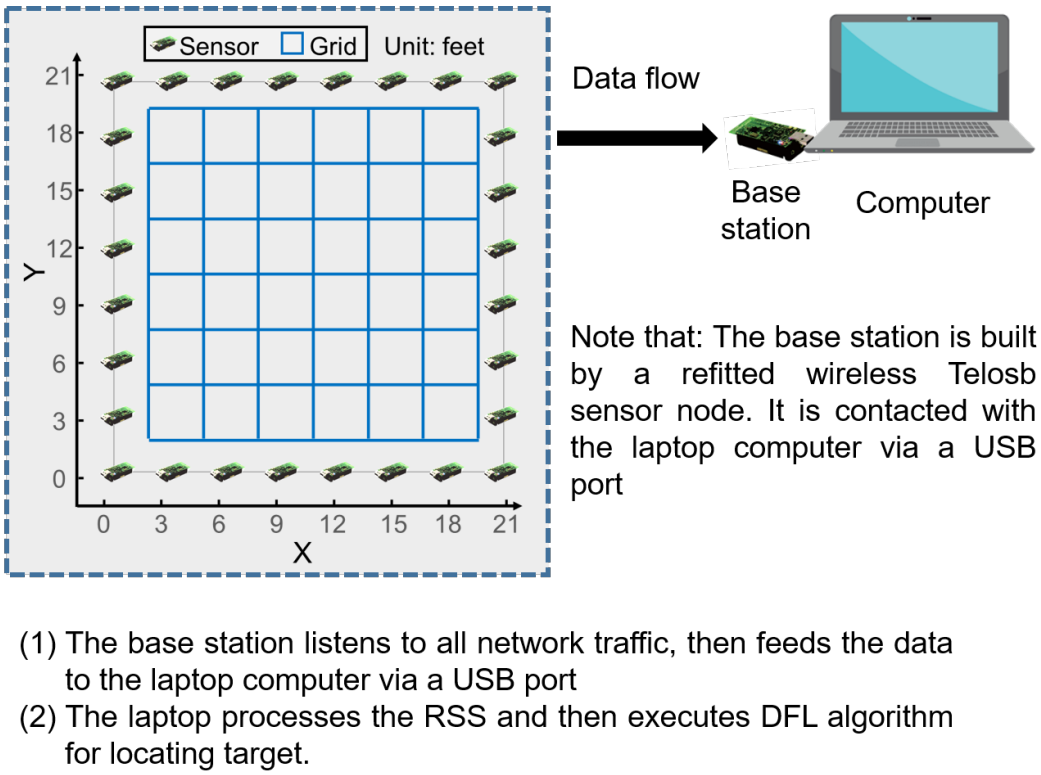

Figure 3.4: Experimental setup of DFL system illustrated as the SPAN Lab of University of Utah [1].

Convolutional Auto-Encoder (CAE) are state-of-the-art for classification and are commonly used in DFL field. Additionally, we also compare the performance of the proposed SC-LR with other two sparse coding algorithms, i.e., Sparse Coding with Orthogonal Matching Pursuit (SC-OMP) and Sparse Coding with Iterative Shrinkage-Thresholding Algorithm (SC-ISTA). SC-OMP and SC-ISTA are with ℓ_0 and ℓ_1 regularization terms, respectively. Both of them are the most famous sparse constraints for DFL [37,38,43,44]. According to the experiment setup of [37,38,43], the original data is used without the preprocess of background elimination.

3.4.3 Other settings and metrics

For a clear presentation on the performance evaluation and comparison, we employ the localization accuracy as a metric to evaluate the performance of all algorithms. It means the percentage of the count of correctly estimated samples to the count of all test samples.

Considering the privacy preservation, we add Gaussian noises in the pure RSS signals to keep the network privacy from leaking to attackers. In addition, in many practical scenarios, DFL system may be unavoidably disturbed by the ambient environment noise. Therefore, the robustness and the signal recovery performance are very important for localization algorithm. Here, we use signal-to-noise-ratio (SNR) to measure the signal quality. SNR is with a definition of $\mathrm{SNR(dB)} = 10\log_{10}(\mathrm{P_{signal}}/\mathrm{P_{noise}})$, where the P_{signal} and P_{noise} denote the signal power and the noise power, respectively.

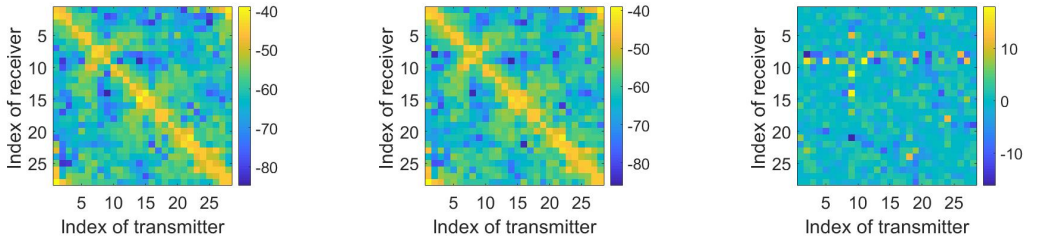

(a) R^{target} (b) R^{vacant} (c) Signal variation, ΔR

Figure 3.5: Example of data pre-processing by background elimination. Here, the example is randomly selected in which the target is at the 11 th grid. Note that, (c) is obtained by signal R^{target} subtracting signal R^{vacant}.

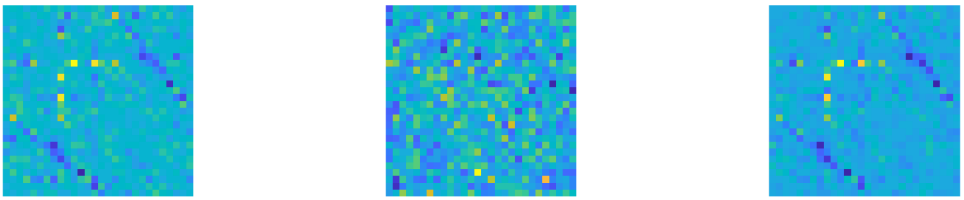

(a) Noiseless testing signal (b) Noisy testing signal (c) Recovery signal

Figure 3.6: Imaging the noiseless testing signal, noisy testing signal and recovery results of the proposed SC-LR algorithm. Here, we present an example when the target is at the 20 th grid of DFL area. The noise level of (b) is with SNR = -10 dB.

3.4.4 Experimental Result and Discussion

3.4.4.1 Data pre-process of background elimination

Since each RSS signal contains many useless signal components that are stronger than the useful signal variation, this results in an adverse effect for classification. For example, the base signal of the background is relatively stable, no matter whether there is an object in the monitoring area or not. Thus, a pre-process of background elimination is necessary. From Fig. 3.5, we perform the pre-process via subtracting the background component $\mathbf{R}^{\text{vacant}}$ from $\mathbf{R}^{\text{target}}$. After this pre-process, many useless signal components can be eliminated. Therefore, the signal variation is apparent with a distinctive feature, as shown in Fig. 3.5(c).

3.4.4.2 Localization performance and comparison

Fig. 3.6 shows the images of the noiseless testing signal, noisy testing signal and recovery results of the proposed SC-LR algorithm. Here, we present the example when the target is at the 20 th grid of the DFL area. The noise level of Fig. 3.6 (b) is with SNR = -10 dB. Considering the high similarity between the original signal and the recovery one, it can be concluded that the proposed algorithm has a strong signal recovery ability. Table 3.1 shows the average localization accuracies obtained by the previously mentioned approaches. In this table, there are three

Table 3.1: Comparison of Localization performance

Noisy testing data (0 dB)	Noisy testing data (-5 dB)	Noisy testing data (-10 dB)
100%	**100**%	**99.4**%
100%	94.0%	51.5%
97.0%	72.7%	30.0%
97.0%	77.9%	40.0%
44.1%	17.1%	13.0%
24.1%	8.0%	3.0%

experimental conditions, including SNR of noisy testing data as 0 dB, -5 dB and -10 dB. From this table, it can be seen that the proposed SC-LR algorithm shows a strong robust performance in the heavy noisy environments for target localization.

3.5 Conclusion

For addressing the problem of device-free localization (DFL) via sparse coding approach, in this paper, we exploit a new log-regularizer in the objective function for classification. With taking the distinctive ability of log-regularizer to measure sparsity, the proposed approach has achieved an accurate localization process with robust performance in the challenging environments.

The experimental results on the real-world dataset show that the proposed approach demonstrates a superior localization performance to that of other compared DFL approaches, especially when the noise in the environment is serious. In detail, the SR-LR can achieve a localization accuracy of 100% when SNR of noisy testing signal is greater than -5 dB. Even when SNR of noisy testing signal equals -10 dB, it can obtain a localization accuracy of 99.4%, which is sufficiently accurate for localization.

Chapter 4

Image Processing-based indoor device-free localization

4.1 Introduction

Since localization has been a hot research topic from the last decade, a great number of work has been developed. Especially for outdoor localization, related positioning techniques are mature such as Global Position System (GPS), Cell Identification (Cell-ID) and Direction or Angle of Arrival (AOA), which can locate the target in an accurate and fast manner. However, the current indoor positioning system cannot achieve the high-precision localization result due to the complex surrounding environment and dense signal interference. For example, the traditional GPS cannot be used for localization in a complex building. Since the GPS signal travels from the satellite, the long-distance leads to the lower−barely GPS signal. Besides, heterogeneous Internet of Things (IoT) with various communication standards (e.g., WiFi, ZigBee and Bluetooth) coexist in the building, which will result in severe signal interference. Moreover, the transmission scenario has a high penetration loss when the signal passes through rooms and stairs, significantly influencing the data quality for localization. As usual, the target must be equipped with a mobile device for indoor localization, which can receive and transmit related signals to the corresponding sides for distance measurement. However, sometimes the target does not carry a mobile device. At this time, the device-free localization technique rises to the surface, which localizes people without any specific devices or is actively involved in the whole process. As shown in Fig. 1, device-free localization consists of Wireless Sensor Networks (WSNs), where a great number of sensors have been deployed in advance for signal collection and analysis [46, 47]. For example, in the application of intrusion detection, once a thief gets into the house, the received signal strength indicator (RSSI) of on-premise sensors will be changed. Subsequently, all the sensing data will be transmitted back to the server, which aggregates all the RSSI and utilizes some pre-trained deep learning networks to find out the current position of the thief. Finally, the administrator will be alerted. Rather than intrusion detection, the device-free localization also have been applied to fall detection and remote monitoring of the elderly, occupancy detection for energy-efficient heating, ventilation, and air conditioning (HVAC) and lighting [48].

However, the different RSS values cannot directly reflect the position informa-

tion of target. Furthermore, the surrounding noise interferes with the signal RSS, deviating the final judgment of location distinction. Hence, we need to transform RSS values into vectors and adopt some deep learning techniques which can exclude noise inference to detect abnormal features more accurately. A great number of machine learning-based work have been proposed to solve the device-free localization problem such as the compressive sensing method [49], radio tomographic imaging (RTI) method [1], an artificial neural network (ANN) method [50] and convolutional neural network (CNN) method [51]. In the above-mentioned techniques, the CNN-based device-free localization is the most attractive since the CNN can fastly extract essential features from a cluster of image pixels and remove the embedded noise, which is helpful for RSS signal modeling and localization confirmation.

Although CNN-based device-free localization can find the target in high precision, some sensors are attacked to the extent that their signal strength values are tampered with, or some sensors are physically damaged and do not work properly. This situation can lead to low accuracy and unreliability in the positioning results. Even worse, the whole system cannot work properly during this period and miss some critical information. To solve this problem, based on the pre-training concept, we propose a CNN-based attack defense for device-free localization. First, deep learning techniques are used to transform the localization problem into an image classification problem. In contrast to traditional algorithms, we design and simulate a partial sensor attack or dropout scenario and train the neural network accordingly. This allows the system to function normally and obtain reliable and relatively accurate localization information even if some sensors are disconnected or attacked. The experiments and analysis show that our algorithm is more resilient to attacks than previous work, and the localization accuracy in the case of partial sensor failure or attack can be guaranteed. The contribution of this paper is illustrated as follows:

1. We propose a CNN-based attack defense for device-free localization, which can defend against sensor dropout and compromised attacks.

2. We utilize the random seed to perturb the training data and generate an anti-interference device-free localization model in the pre-training stage.

3. The experiment results on a real-world dataset verify that our proposed scheme can still achieve the accurate localization result in case of potential attacks.

4.1.1 Organization of this paper

The rest of this paper is organized as follows. Section 2 illustrates the related works about device-free localization. In Section 3, we formulate the DFL problem as a classification problem and also devise the BE scheme. Section 4 presents the algorithm. Section 5 evaluates the performance of our proposal. Finally, this work is concluded in Section 6.

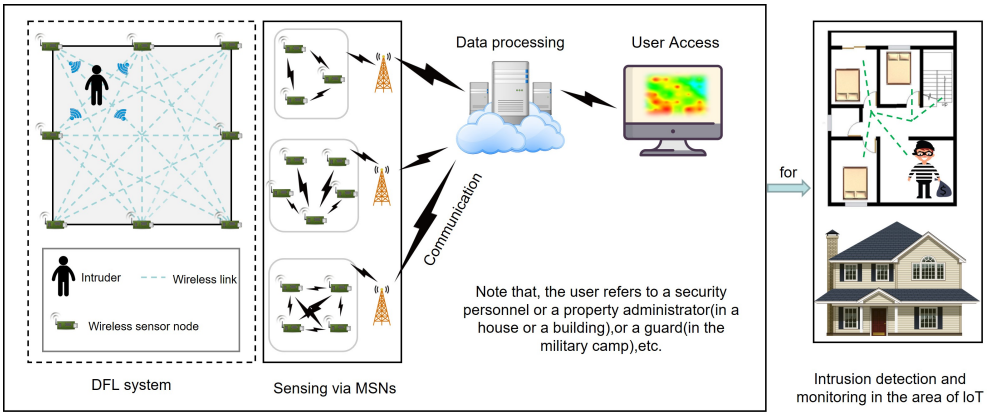

Figure 4.1: Traditional device-free localization framework.

4.2 Related work

The concept of device-free localization has been proposed by Youssef et al. [52], which analyzed dynamic RF signals changed by the object movement in the environment and correlate their locations. To achieve better localization performance, in a real environment, Moussa et al. [53] modelled the localization problem into a fingerprint identification problem, which was solved by a new algorithm based on Maximum Likelihood Estimator (MLE) and improved the performance of initial device-free localization system. Wilson et al. [1] firstly used radio tomographic imaging to extract the attenuation of RF wavelength when penetrating physical objects. The proposed method is able to realize the RF attenuation for object localization. Zhang et al. [54] proposed a new device-free object tracking system called RASS, which transforms the tracking field into various triangle areas and multiple channels are used to mitigate noise interference among different nodes. Seifeldin et al. [55] presented Nuzzer device free localization system, which utilized RSS variance to measure the number of entities in the target area and find the exact position of these objects. Based on real-environment data sensing from surroundings, Guo et al. [56] proposed the RSS model, which consists of small-scale reayleigh enhancement part and large-scale exponential attenuation part. The experiment results show their proposed framework can solve the unpredictable device-free localization issue resulted from the multipath interference. Wang et al. [57] designed a novel BGA framework, which consists of shadowed links and the prior information in the estimation period. The proposed BGA framework shows a good performance that tracking error is greatly reduced in the device-free localization phase. Ciuonzo et al. [58] utilized sensors to measure a random signal resulted from the distance between transmitter and the receiver, and then sent to a fusion centre for device-free detection performance improvement. For decentralized device-free detection, Ciuonzo et al. [59] proposed a general version of Rao test arises from maximization of Rao decision statistics family, which can improve the previous performance of device-free localization. Sabek et al. [60] transformed multi-agent device free localization problem into an energy-minimization framework, which can maintain temporal and spatial smoothness and consistency. The proposed solution can map the localization problem into a binary graph-cut problem. Moreover, the noise and accuracy are reduced and enhanced by the clustering

techniques, respectively. Xiao et al. [61] designed a CSI-based passive device-free localization system called Pilot, which makes use of the features of CSI to monitor the abnormal information. Especially, the three blocks design can increase the efficiency of passive device free localization problem. Wu et al. Wu et al. [62] proposed FILA, which is cross-layer method that can achieve the aim of high accurate indoor localization in WLANs, which includes two parts: CSI-based propagation model and CSI-based fingerprinting. The FILA is implemented in commodity 802.11 NICs and the experiment evaluates the correctness and feasibility of proposed method. Wang et al. [50] proposed a deep-learning-based indoor fingerprint framework according to the CSI value. Besides, the offline training and online localization phases. The experiment result shows the proposed method can achieve good performance under signal propagation environments.

4.3 Problem Statement

4.3.1 Device-free localization problem illustration

As shown in Fig. 4.1, D wireless sensor nodes which compose of the monitoring area sense the signal strength from the target and figure out the current position. Note that all the sensors transmit and receive wireless signals in turn. At the beginning time, there is no object in the system, so the RSS matrix derived from the RSS matrix is empty, which can be defined as RSS^{null}. As we know the number of wireless sensor is D, the RSS measurement can be computed as $D \times D$. If the target enters into the measurement area, the total RSS matrix from all the wireless sensors can be computed as RSS^{target}. Note that the RSS value from the ith sensor to the jth sensor can be defined as $RSS_{i,j}^{target}$, whose summation derives the RSS^{target}. As we have mentioned, if the target is not in the target area, the RSS^{target} will be 0. When the target appears in the detection area, the surrounding signal transmitted and received by the corresponding sensors will be greatly influenced. For example, the initial value of 5th sensor is RSS_5^{null} will be changed to RSS_5^{target}. Since the feature of RSS value has strong connection with the target position, the object can be localized by the RSS measurements at the end of device side. In the following subsections, we will talk more details about this transformation.

4.3.2 Problem modelling

The target localization problem can be transformed into RSS matrix computation. From the Fig. 4.1, we firstly collect the signal strength from all the sensors under two circumstances (e.g., target non-existence and target existence). Note that the significant components of the signal are extracted by the background elimination method. Note that the background elimination can make the features of matrice variation more obvious. The signal variation can be formulated as: $\Delta RSS_{i,i} = RSS_{i,j}^{\text{target}} - RSS_{i,j}^{\text{empty}}$. After collecting all data from the sensors, the

RSS matrix can be established as:$\Delta RSS = \begin{bmatrix} \Delta RSS_{1,1} & \Delta RSS_{1,2} & \cdots & \Delta RSS_{1,D} \\ \Delta RSS_{2,1} & \Delta RSS_{2,2} & \cdots & \Delta RSS_{2,D} \\ \Delta RSS_{3,1} & \Delta RSS_{3,2} & \cdots & \Delta RSS_{3,D} \\ \vdots & \vdots & \ddots & \vdots \\ \Delta RSS_{D,1} & \Delta RSS_{D,2} & \cdots & \Delta RSS_{D,D} \end{bmatrix}$.
We can observe from the ΔRSS, RSS matrices can reflect the features of each target position. Once we consider the RSS matrix as the image matrix, we can transform object localization issue into image identification problem. Especially the different hot spots derived from the matrices can directly show the variations of RSS value. The feature image obtained from the RSS matrices also owns the same patterns for target position recognition. Hence, we can utilize some traditional image process technique such as CNN and ResNet to figure out the exact position of target.

4.3.3 Data collection

For easy measurement, we divide the whole sensing area into many small sections, which can be regarded as a class. T grids compose of T classes for image identification problem. The training data for target localization can be constructed as $V = [V_{11}, V_{12}..., V_{TP}]$, where p means that the number of experiment times. Note that $V_s(s = 1, 2, ..., S)$ is the training dataset.

4.3.4 Potential attack

In this venue, we assume a potential attacker would like to interfere sensing data collection or crack some normal devices for the entire system. To simulate the behaviours the adversary, we replace some random RSS value with training data, which is transformed to $\Delta RSS' = \begin{bmatrix} \Delta RSS'_{1,1} & \Delta RSS'_{1,2} & \cdots & \Delta RSS'_{1,D} \\ \Delta RSS'_{2,1} & \Delta RSS'_{2,2} & \cdots & \Delta RSS'_{2,D} \\ \Delta RSS'_{3,1} & \Delta RSS'_{3,2} & \cdots & \Delta RSS'_{3,D} \\ \vdots & \vdots & \ddots & \vdots \\ \Delta RSS'_{D,1} & \Delta RSS'_{D,2} & \cdots & \Delta RSS'_{D,D} \end{bmatrix}$.
Note that $\Delta RSS'$ means the RSS value after interference. Subsequently, the training set also will be changed to $V' = [V'_{11}, V'_{12}..., V'_{TP}]$. Hence, in our proposed method, we should conduct device-free localization even under attack scenario accurately.

4.4 Proposed Method

CNN is a powerful tool to process image and has been applied to many application fields such as facial recognition, documents analysis and climate estimation. In our proposed framework, we also utilize the CNN to train a device-free localization model in the pre-training process including normal data for attack defense. The detailed process is illustrated as follows:

1. Firstly, all the wireless sensors send and receive the signals from the remaining sensors collaboratively. If no object enters in the monitoring area, the

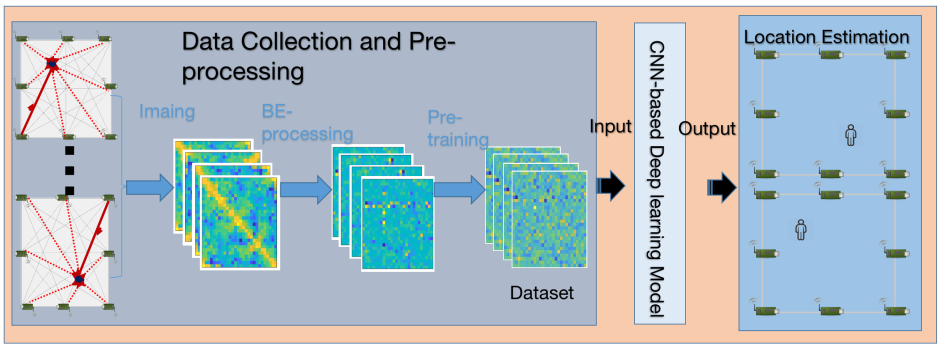

Figure 4.2: Detailed process of our proposed method.

RSS received by the each sensor will be a constant value $RSS_{i,j}^{Null}$. Once an object appears, the RSS will be changed into another value which is obviously different from the $RSS_{i,j}^{Null}$ as $RSS_{i,j}^{target}$. After aggregating all the $RSS_{i,j}^{target}$, we start to analyse the exact location of target.

2. Since some useless noise is included in the received $RSS_{i,j}^{target}$, the original signal may be interfered for further analysis. As shows in Fig. 4.2, when a set of $RSS_{i,j}^{target}$ is presented in the image format, the background color is very obvious and even may affect the judgement of object localization features. Hence, we need to apply some image pre-processing technique to removing these unnecessary factors. Background elimination (BE) is a widely used approach to remove background element and reduce storage cost. Thus, we utilize the BE technique to handle our figures as $\Delta RSS_{i,i} = RSS_{i,j}^{\text{target}} - RSS_{i,j}^{\text{empty}}$, where $\Delta RSS_{i,i}$ can reflect the significant location features of the object in some degree.

3. Since the whole monitoring area has been divided into some grids, the location dataset can be represented as $V = [V_{11}, V_{12}...V_{lp}...VLP]$. Then, we can apply the CNN technique to establishing the device-free localization model in the pre-training process. As shown in Fig. 4.2 , two-dimensional kernels in the convolution layer will scan the whole space in the source image to extract features, which will be the input for the subsample layer. Subsampling can reduce the reliance of precise positioning within feature maps and construct a more accurate device-free localization model. The related formulation is $\boldsymbol{y}_s = f(\boldsymbol{c} + \boldsymbol{W} * \boldsymbol{U})$, where W and c are the parameters in the convolutional layer, $*$ means the convolution operation. $f(\cdot)$ refers to the rectified linear unite (ReLU) as $f(z) = max(0, z)$, where z is obtained by the each layer. Besides, we also adopt the filter concatenation method to extract features of different data. The final classification performance can be improved by this filter. The previous mentioned sub-sampling is executed by the max pooling and dropout can decrease the positives of

some neural, which can avoid over-fitting situation in possible. Note that the cross-entropy error function is adopted in our framework to update our model as $(\boldsymbol{W}, \boldsymbol{c}) = \frac{1}{S}\sum_{s=1}^{S} \boldsymbol{y}_s \times \log(\boldsymbol{y}'_s(\boldsymbol{W}, \boldsymbol{c}))$, where y'_s, y_s, J means the model prediction, label value and corss-entropy error. Finally, we get a device-free localization model in the pre-training process.

4. In our assumed scenario, an adversary tries to interfere the received RSS value at each sensor's side or some sensors may be compromised. To simulate the behaviours of adversary, we add some random data into the partial training. Hence, RSS value will be changed to $\Delta RSS'$ and the corresponding dataset turns V'. Then we use the pre-trained device free detection model to recognize the abnormal data. After a few turns training, the previous localization model can be transformed into the attack defense device-free localization model.

5. When a real adversary tries to conduct some attacks, the attack defense device-free localization model can fastly and accurate exclude the adverbial interference and localize the object without error.

The detailed process of method is illustrated in 4.2.

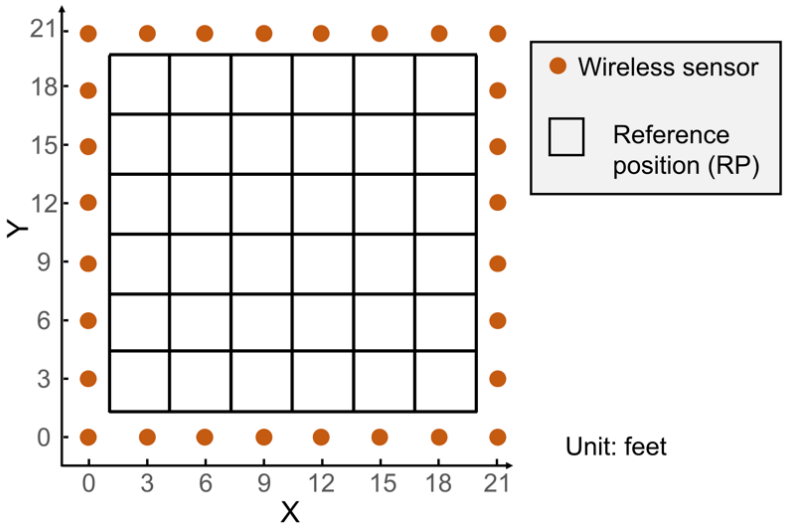

Figure 4.3: The experiment layout for device-free localization scenario for the used dataset.

4.5 Performance Evaluation

In this section, we evaluate the performance of our proposed CNN attack defense device-free localization model under on a real-world dataset collected by the SPANLab of University of Utah. The experiments are conducted on ere performed in the tensorFlow 1.15.0 open source software, which is on the windows 10 operation system with a Tesla T4 GPU and 16 GB of memory.

4.5.1 Dataset description

In the used dataset, wireless sensor network consists of Crossbow TelosB nodes, whose protocol and frequency band are 2.4 GHz and IEEE 802.15.4, respectively. Moreover, this node takes the role of base station for data collection and process. From the figure. 4.3 , we can see the monitoring area is divided into 36 grids consisting of 28 TelosB nodes, whose total area is 21 × 21. Besides, the distance between two adjacent nodes is three feet. In our experiment, when a target enters into range, the total measurement times for RSSI value is 30. The obtained training dataset is 25 samples, the testing data is 5, and the total selected reference points are 36. Moreover, the following equation is used to evaluate the accuracy of all the models: Accuracy $= \frac{C_{\text{correct}}}{C_{\text{total}}} \times 100\%$. The detailed reference point distribution can be referred to Fig. 4.3. Note that the noise is embedded into original dataset for attack-defense device-free localization method during the pre-training process.

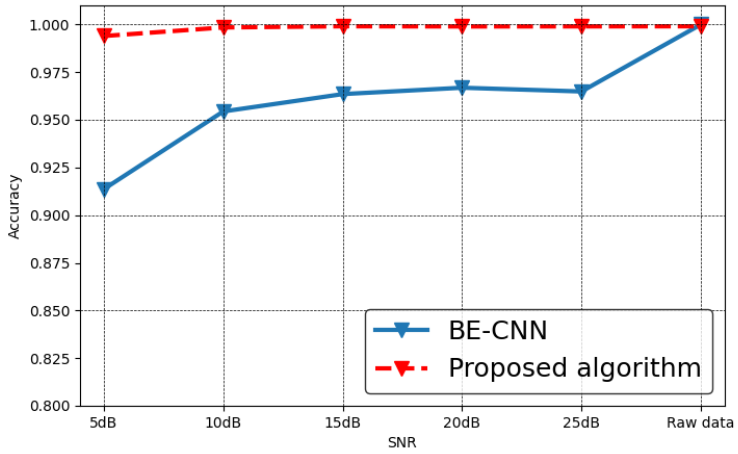

Figure 4.4: Localization accuracy for BE-CNN and our proposed device free localization method.

4.5.2 Attack-defense parameter setting

For our attack-defense device free localization, we need to obtain some optimized parameters (i.e., the number of filters, the number of convolutional layers, sub-sampling layers and kernel size) for CNN training. According to the expected result from the attack-defense localization method, we can get the optimal parameters for our method, which is 2 convolutional layers, 9*9 concatenated convolutional filter size, 32 filter number for each layer, 100 epoches, 10^{-4} learning rate, 300 batch size and 0.4 dropout rate for avoiding overfitting.

4.5.3 Method performance

Our proposed attack-defense device-free localization protocol is trained in the pre-training process, where some random noise are replaced with normal RSS valune. To evaluate the performance between our proposed CNN-based attack

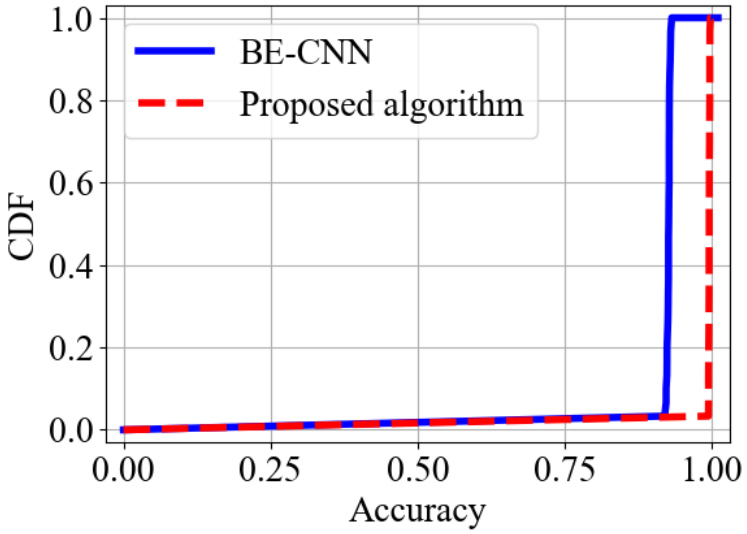

Figure 4.5: Cumulative distribution function (CDF) for our method and BE-CNN for device-free localization.

defense device free localization method and BE-CNN, we need to adjust the signal-noise-rate for comparison. Firstly, we evaluate the converge rate for our proposed method and BE-CNN [29] under different noise distribution, where the related experiments are conducted on fix number of sensors. Moreover, we set the distance for two adjacent for two is 12 feet. As can be seen from Fig. 4.4, when there is no noise interference in the environment, both our proposed protocol and BE-CNN can achieve the 100% localization accuracy rate. When the noise level is increased, our proposed protocol can still achieve the accuracy which is still close to 100%. However, the localization accuracy for BE-CNN is suddenly decreased when the SNR is adjusted to a low value. When the SNR arrives the 5db, the BE-CNN can only achieve 90 % accuracy rate compared with the nearly 100% that our proposed attack-defense device-free localization method. Moreover, we also conduct the experiment to test the cumulative distribution function (CDF) performance for BE-CNN and our proposed attack defense device free localization method under 5 db. As shown in Fig. 4.5, after 30 times experiment, our proposed method can always achieve 100% localization accuracy which is better than the performance achieved by BE-CNN in general. Finally, to evaluate the necessities and superiority for our selected CNN-based attack defense for device free localization, we also change the deep learning method to SVM and KNN. From the Fig. 4.6, the result shows that our proposed CNN-based attack defense method can achieve the 100% localization accuracy which is better than 89% and 51% achieved by the SVM and KNN, respectively. From the above-mentioned multiple performance evaluation experiments, we can see our proposed CNN-based device free localization protocol can defend sever noise interference and achieve the good localization accuracy.

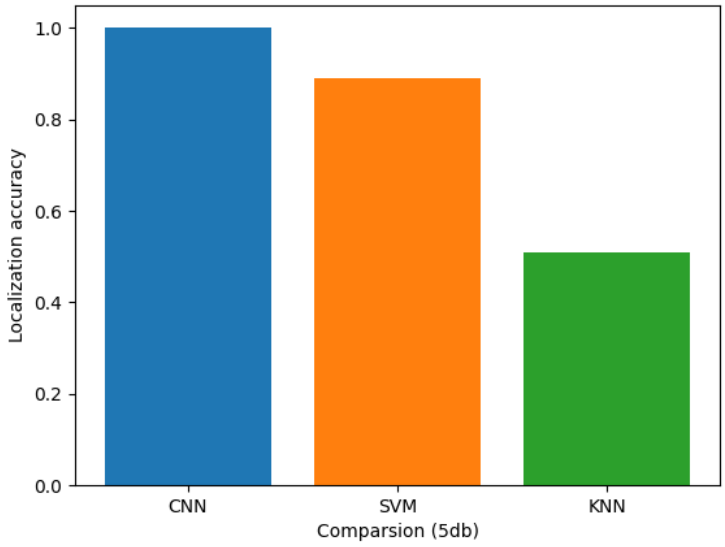

Figure 4.6: Accuracy comparison of different deep learning techniques for device free localization.

4.6 Conclusion and Future work

To defend potential device compromised and sever signal interference during device-free localization, we propose a CNN-based attack defense device-free localization method in this paper. The multiple experiments verify that our proposed method can achieve better localization accuracy compared with other deep learning-based technique and defend mostly possible attacks [63,64]. In the future work, we will explore the popular CNN framework such as AlexNet or ResNet, which can maintain the localization accuracy under more sever circumstances.

Chapter 5

Conclusions and Future work

5.1 Conclusions

In this dissertation, we firstly propose a new algorithm to integrate indoor target positioning and communication based on the features of WiFi signal. The method for realizing indoor positioning and communication based on WiFi signals is of practical significance, and it is not difficult to implement and the cost is low. The RSS and CSI values in the WiFi signal are used to achieve indoor target positioning respectively, and the derived indoor wireless channel system transfer function is used to achieve the purpose of communication. In the positioning part based on the RSS value, the accuracy of the algorithm can reach 0.25m, which can meet the indoor positioning requirements under certain conditions.

Given in some scenarios, the target may not expect to be equipped with extra devices. Therefore, we formulate device-free localization issue as the classification problem and exploit a log regularizer in the objective function for classification.For addressing the problem of device-free localization (DFL) via sparse coding approach, in this paper, we exploit a new log-regularizer in the objective function for classification. With taking the distinctive ability of log-regularizer to measure sparsity, the proposed approach has achieved an accurate localization process with robust performance in the challenging environments.

5.2 Future work

In future research we will continue to work on indoor localization, as the channel state information CSI can provide more detailed and specific carrier counts. We will try to build an experimental platform to collect CSI from different locations, and then try to solve the indoor DFL problem by using the classification methods covered in this thesis, sparse coding and CNN and other networks on them. On the other hand, we will design some multi-target identification schemes and experiments using the CSI characteristics to solve the indoor multi-target localization problem.

References

[1] J. Wilson and N. Patwari, "Radio tomographic imaging with wireless networks," *IEEE Transactions on Mobile Computing*, vol. 9, no. 5, pp. 621–632, 2010.

[2] Z. Huang, X. Zhu, Y. Lin, L. Xu, and Y. Mao, "A novel wifi-oriented rssi signal processing method for tracking low-speed pedestrians," in *2019 5th International Conference on Transportation Information and Safety (ICTIS)*. IEEE, 2019, pp. 1018–1023.

[3] S. Tabatabaei, "A novel fault tolerance energy-aware clustering method via social spider optimization (sso) and fuzzy logic and mobile sink in wireless sensor networks (wsns)." *Comput. Syst. Sci. Eng.*, vol. 35, no. 6, pp. 477–494, 2020.

[4] R. Ma, Q. Guo, C. Hu, and J. Xue, "An improved wifi indoor positioning algorithm by weighted fusion," *Sensors*, vol. 15, no. 9, pp. 21 824–21 843, 2015.

[5] B. Wang, X. Liu, B. Yu, R. Jia, and X. Gan, "An improved wifi positioning method based on fingerprint clustering and signal weighted euclidean distance," *Sensors*, vol. 19, no. 10, p. 2300, 2019.

[6] Z.-A. Deng, G. Wang, D. Qin, Z. Na, Y. Cui, and J. Chen, "Continuous indoor positioning fusing wifi, smartphone sensors and landmarks," *Sensors*, vol. 16, no. 9, p. 1427, 2016.

[7] C.-H. Hsieh, J.-Y. Chen, and B.-H. Nien, "Deep learning-based indoor localization using received signal strength and channel state information," *IEEE access*, vol. 7, pp. 33 256–33 267, 2019.

[8] N. Yu, S. Zhao, X. Ma, Y. Wu, and R. Feng, "Effective fingerprint extraction and positioning method based on crowdsourcing," *IEEE Access*, vol. 7, pp. 162 639–162 651, 2019.

[9] S. Lembo, S. Horsmanheimo, M. Somersalo, M. Laukkanen, L. Tuomimäki, and S. Huilla, "Enhancing wifi rss fingerprint positioning accuracy: lobe-forming in radiation pattern enabled by an air-gap," in *2019 International Conference on Indoor Positioning and Indoor Navigation (IPIN)*. IEEE, 2019, pp. 1–8.

[10] G. Guo, R. Chen, F. Ye, X. Peng, Z. Liu, and Y. Pan, "Indoor smartphone localization: A hybrid wifi rtt-rss ranging approach," *IEEE Access*, vol. 7, pp. 176 767–176 781, 2019.

[11] H. Shu, C. Song, T. Pei, L. Xu, Y. Ou, L. Zhang, and T. Li, "Queuing time prediction using wifi positioning data in an indoor scenario," *Sensors*, vol. 16, no. 11, p. 1958, 2016.

[12] W. Yang, L. Gong, D. Man, J. Lv, H. Cai, X. Zhou, and Z. Yang, "Enhancing the performance of indoor device-free passive localization," *Int. J. Distrib. Sens. Netw.*, vol. 11, no. 11, p. 256162, 2015.

[13] D. G. Michelson, N. T. Golmie, C. Gentile, J. T. Quimby, K. A. Remley, Y. de Jong, and K. Gracie, "A classification scheme for wireless channel models across the development life cycle," in *2019 USNC-URSI Radio Science Meeting (Joint with AP-S Symposium)*. IEEE, 2019, pp. 47–48.

[14] A. Kumar, R. Bhattacharjee, and S. Goel, "A clustering based channel model for indoor wireless communication," in *2011 National Conference on Communications (NCC)*. IEEE, 2011, pp. 1–5.

[15] R. Xu, L. Wang, Z. Geng, H. Deng, L. Peng, and L. Zhang, "A unitary precoder for optimizing spectrum and papr characteristic of ofdma signal," *IEEE Transactions on Broadcasting*, vol. 64, no. 2, pp. 293–306, 2017.

[16] A. A. Kalachikov and N. S. Shelkunov, "Construction and validation of analytical wireless mimo channel models based on channel measurement data," in *2018 XIV International Scientific-Technical Conference on Actual Problems of Electronics Instrument Engineering (APEIE)*. IEEE, 2018, pp. 175–179.

[17] R. Stridh, K. Yu, B. Ottersten, and P. Karlsson, "Mimo channel capacity and modeling issues on a measured indoor radio channel at 5.8 ghz," *IEEE Transactions on Wireless Communications*, vol. 4, no. 3, pp. 895–903, 2005.

[18] X. Liu, C. Liu, W. Liu, and X. Zeng, "Wireless channel modeling and performance analysis based on markov chain," in *2017 29th Chinese Control And Decision Conference (CCDC)*. IEEE, 2017, pp. 2256–2260.

[19] Y. Zhang, L. Hsiung-Cheng, J. Zhao, M. Zewen, Z. Ye, and H. Sun, "A multi-dof ultrasonic receiving device for indoor positioning of agv system," in *2018 International Symposium on Computer, Consumer and Control (IS3C)*. IEEE, 2018, pp. 97–100.

[20] F. Gonzalez, F. Gosselin, and W. Bachta, "A 2-d infrared instrumentation for close-range finger position sensing," *IEEE Transactions on Instrumentation and Measurement*, vol. 64, no. 10, pp. 2708–2719, 2015.

[21] M. U. Ali, S. Hur, and Y. Park, "Wi-fi-based effortless indoor positioning system using iot sensors," *Sensors*, vol. 19, no. 7, p. 1496, 2019.

[22] H. Xu, Y. Ding, P. Li, R. Wang, and Y. Li, "An rfid indoor positioning algorithm based on bayesian probability and k-nearest neighbor," *Sensors*, vol. 17, no. 8, p. 1806, 2017.

[23] C. Yang and H.-R. Shao, "Wifi-based indoor positioning," *IEEE Communications Magazine*, vol. 53, no. 3, pp. 150–157, 2015.

[24] A. Noertjahyana, I. A. Wijayanto, and J. Andjarwirawan, "Development of mobile indoor positioning system application using android and bluetooth low energy with trilateration method," in *2017 international conference on soft computing, intelligent system and information technology (ICSIIT)*. IEEE, 2017, pp. 185–189.

[25] S. Lee, Y. Ahn, and H. Y. Kim, "Predicting concrete compressive strength using deep convolutional neural network based on image characteristics," *CMC-COMPUTERS MATERIALS & CONTINUA*, vol. 65, no. 1, pp. 1–17, 2020.

[26] M. Khan and M. K. Jain, "Feature point detection for repacked android apps [j]," *Intelligent Automation and Soft Computing*, vol. 26, no. 4, pp. 1359–1373, 2020.

[27] F. Yucel and E. Bulut, "Clustered crowd gps for privacy valuing active localization," *IEEE Access*, vol. 6, pp. 23 213–23 221, 2018.

[28] M. Scherhäufl, M. Pichler, and A. Stelzer, "Uhf rfid localization based on phase evaluation of passive tag arrays," *IEEE Transactions on Instrumentation and Measurement*, vol. 64, no. 4, pp. 913–922, 2015.

[29] L. Zhao, C. Su, H. Huang, Z. Han, S. Ding, and X. Li, "Intrusion detection based on device-free localization in the era of iot," *Symmetry*, vol. 11, no. 5, p. 630, 2019.

[30] A. Booranawong, N. Jindapetch, and H. Saito, "Adaptive filtering methods for rssi signals in a device-free human detection and tracking system," *IEEE Systems Journal*, 2019.

[31] D. Konings, F. Alam, F. Noble, and E. M. Lai, "Springloc: A device-free localization technique for indoor positioning and tracking using adaptive rssi spring relaxation," *IEEE Access*, vol. 7, pp. 56 960–56 973, 2019.

[32] H. Huang, S. Guo, P. Li, and T. Miyazaki, "Stochastic analysis on the deactivation-controlled epidemic routing in dtns with multiple sinks," *Ad hoc and sensor wireless networks*, 2017.

[33] H. Huang, S. Guo, W. Liang, K. Wang, and A. Y. Zomaya, "Green data-collection from geo-distributed iot networks through low-earth-orbit satellites," *IEEE Transactions on Green Communications and Networking*, 2019.

[34] Z. Li, Z. Yang, S. Xie, W. Chen, and K. Liu, "Credit-based payments for fast computing resource trading in edge-assisted internet of things," *IEEE Internet of Things Journal*, 2019.

[35] H. Huang and S. Guo, "Proactive failure recovery for nfv in distributed edge computing," *IEEE Communications Magazine*, vol. 57, no. 5, pp. 131–137, 2019.

[36] L. Zhao, H. Huang, S. Ding, and X. Li, "An accurate and efficient device-free localization approach based on gaussian bernoulli restricted boltzmann machine," in *2018 IEEE International Conference on Systems, Man, and Cybernetics (SMC)*. IEEE, 2018, pp. 2323–2328.

[37] H. Huang, H. Zhao, X. Li, S. Ding, L. Zhao, and Z. Li, "An accurate and efficient device-free localization approach based on sparse coding in subspace," *IEEE Access*, vol. 6, no. 1, pp. 61 782–61 799, 2018.

[38] D. Wang, X. Guo, and Y. Zou, "Accurate and robust device-free localization approach via sparse representation in presence of noise and outliers," in *IEEE International Conference on Digital Signal Processing (DSP)*. IEEE, 2016, pp. 199–203.

[39] H. Huang, Z. Han, S. Ding, C. Su, and L. Zhao, "Improved sparse coding algorithm with device-free localization technique for intrusion detection and monitoring," *Symmetry*, vol. 11, no. 5, p. 637, 2019.

[40] Y. Han, X.-C. Feng, G. Baciu, and W.-W. Wang, "Nonconvex sparse regularizer based speckle noise removal," *Pattern Recognition*, vol. 46, no. 3, pp. 989–1001, 2013.

[41] C. A. Micchelli, J. M. Morales, and M. Pontil, "Regularizers for structured sparsity," *Advances in Computational Mathematics*, vol. 38, no. 3, pp. 455–489, 2013.

[42] Z. Li, S. Ding, Y. Li, Z. Yang, S. Xie, and W. Chen, "Manifold optimization-based analysis dictionary learning with an $l_{1/2}$-norm regularizer," *Neural Networks*, vol. 98, pp. 212–222, 2018.

[43] T. Liu, X. Luo, and Z. Liang, "Enhanced sparse representation-based device-free localization with radio tomography networks," *Journal of Sensor and Actuator Networks*, vol. 7, no. 1, p. 7, 2018.

[44] J. Wang, X. Zhang, Q. Gao, H. Yue, and H. Wang, "Device-free wireless localization and activity recognition: A deep learning approach," *IEEE Transactions on Vehicular Technology*, vol. 66, pp. 6258–6267, 2017.

[45] L. Zhao, H. Huang, X. Li, S. Ding, H. Zhao, and Z. Han, "An accurate and robust approach of device-free localization with convolutional autoencoder," *IEEE Internet of Things Journal*, 2019.

[46] W. Wang, G. Srivastava, J. C.-W. Lin, Y. Yang, M. Alazab, and T. R. Gadekallu, "Data freshness optimization under caa in the uav-aided mecn: A potential game perspective," *IEEE Transactions on Intelligent Transportation Systems*, 2022.

[47] T. Wang, Y. Quan, X. S. Shen, T. R. Gadekallu, W. Wang, and K. Dev, "A privacy-enhanced retrieval technology for the cloud-assisted internet of things," *IEEE transactions on industrial informatics*, 2021.

[48] F. Alam, N. Faulkner, and B. Parr, "Device-free localization: A review of non-rf techniques for unobtrusive indoor positioning," *IEEE Internet of Things Journal*, vol. 8, no. 6, pp. 4228–4249, 2020.

[49] L. Chang, X. Chen, Y. Wang, D. Fang, J. Wang, T. Xing, and Z. Tang, "Fitloc: Fine-grained and low-cost device-free localization for multiple targets over various areas," *IEEE/ACM Transactions on Networking*, 2017.

[50] X. Wang, L. Gao, and S. Mao, "Csi phase fingerprinting for indoor localization with a deep learning approach," *IEEE Internet Things J.*, vol. 3, no. 6, pp. 1113–1123, 2016.

[51] X. Wang, X. Wang, and S. Mao, "Deep convolutional neural networks for indoor localization with csi images," *IEEE Trans. Netw. Sci. Eng.*, 2018.

[52] M. Youssef, M. Mah, and A. Agrawala, "Challenges: device-free passive localization for wireless environments," in *Proceedings of the 13th annual ACM international conference on Mobile computing and networking*. ACM, 2007, pp. 222–229.

[53] M. Moussa and M. Youssef, "Smart cevices for smart environments: Device-free passive detection in real environments," in *Pervasive Computing and Communications, 2009. PerCom 2009. IEEE International Conference on*. IEEE, 2009, pp. 1–6.

[54] D. Zhang, Y. Liu, X. Guo, and L. M. Ni, "Rass: A real-time, accurate, and scalable system for tracking transceiver-free objects," *IEEE Transactions on Parallel and Distributed Systems*, vol. 24, no. 5, pp. 996–1008, 2012.

[55] M. Seifeldin, A. Saeed, A. E. Kosba, A. El-Keyi, and M. Youssef, "Nuzzer: A large-scale device-free passive localization system for wireless environments," *IEEE Transactions on Mobile Computing*, vol. 12, no. 7, pp. 1321–1334, 2012.

[56] Y. Guo, K. Huang, N. Jiang, X. Guo, Y. Li, and G. Wang, "An exponential-rayleigh model for rss-based device-free localization and tracking," *IEEE transactions on mobile computing*, vol. 14, no. 3, pp. 484–494, 2014.

[57] J. Wang, Q. Gao, P. Cheng, Y. Yu, K. Xin, and H. Wang, "Lightweight robust device-free localization in wireless networks," *IEEE transactions on industrial electronics*, vol. 61, no. 10, pp. 5681–5689, 2014.

[58] D. Ciuonzo and P. S. Rossi, "Distributed detection of a non-cooperative target via generalized locally-optimum approaches," *Information Fusion*, vol. 36, pp. 261–274, 2017.

[59] D. Ciuonzo, P. S. Rossi, and P. Willett, "Generalized rao test for decentralized detection of an uncooperative target," *IEEE Signal Processing Letters*, vol. 24, no. 5, pp. 678–682, 2017.

[60] I. Sabek, M. Youssef, and A. V. Vasilakos, "Ace: An accurate and efficient multi-entity device-free wlan localization system," *IEEE transactions on mobile computing*, vol. 14, no. 2, pp. 261–273, 2014.

[61] J. Xiao, K. Wu, Y. Yi, L. Wang, and L. M. Ni, "Pilot: Passive device-free indoor localization using channel state information," in *Distributed computing systems (ICDCS), 2013 IEEE 33rd international conference on.* IEEE, 2013, pp. 236–245.

[62] K. Wu, J. Xiao, Y. Yi, D. Chen, X. Luo, and L. M. Ni, "Csi-based indoor localization," *IEEE Transactions on Parallel and Distributed Systems*, vol. 24, no. 7, pp. 1300–1309, 2012.

[63] J. Jiang, F. Liu, W. W. Ng, Q. Tang, W. Wang, and Q.-V. Pham, "Dynamic incremental ensemble fuzzy classifier for data streams in green internet of things," *IEEE Transactions on Green Communications and Networking*, 2022.

[64] Y. Yang, W. Wang, L. Liu, K. Dev, and N. M. F. Qureshi, "Aoi optimization in the uav-aided traffic monitoring network under attack: A stackelberg game viewpoint," *IEEE Transactions on Intelligent Transportation Systems*, 2022.